

Cellular origin of bladder neoplasia and tissue dynamics of its progression to invasive carcinoma

Kunwoo Shin^{1,8}, Agnes Lim², Justin I. Odegaard³, Jared D. Honeycutt⁴, Sally Kawano¹, Michael H. Hsieh⁵ and Philip A. Beachy^{1,2,6,7,8}

Understanding how malignancies arise within normal tissues requires identification of the cancer cell of origin and knowledge of the cellular and tissue dynamics of tumour progression. Here we examine bladder cancer in a chemical carcinogenesis model that mimics muscle-invasive human bladder cancer. With no prior bias regarding genetic pathways or cell types, we prospectively mark or ablate cells to show that muscle-invasive bladder carcinomas arise exclusively from Sonic hedgehog (*Shh*)-expressing stem cells in basal urothelium. These carcinomas arise clonally from a single cell whose progeny aggressively colonize a major portion of the urothelium to generate a lesion with histological features identical to human carcinoma *in situ*. *Shh*-expressing basal cells within this precursor lesion become tumour-initiating cells, although *Shh* expression is lost in subsequent carcinomas. We thus find that invasive carcinoma is initiated from basal urothelial stem cells but that tumour cell phenotype can diverge significantly from that of the cancer cell of origin.

The idea that human malignancies may originate from adult tissue stem cells derives from the intrinsic ability of stem cells to self-renew, from their longevity and consequent ability to accrue multiple mutations, and from the phenotypic resemblance of tumour-propagating cells to tissue stem cells^{1–4}. Experimental tests of this hypothesis, however, have revealed a surprising degree of complexity⁵. Recent mouse studies using cell-specific genetic manipulation have produced evidence that ovarian cancer, glioblastoma, skin cancer and intestinal adenomas/carcinomas are derived from tissue stem cells^{6–10}, but other studies have suggested that luminal epithelial cells may serve as the cancer cell of origin. Thus, in mouse mammary tissue, tumours of greatest histological similarity to human mammary adenocarcinoma arise on Cre-mediated deletion of *Brca1/Trp53* in luminal cells, even though aggressive human mammary tumours are phenotypically basal in character^{11,12}. Similarly, with oncogene expression and transplantation into the murine kidney capsule as an assay, prostate adenocarcinoma arises exclusively from basal cells of mouse^{13,14} or human¹⁵ prostate whereas autochthonous adenocarcinomas caused by deletion of *PTEN* can arise from either basal or luminal cells^{16,17}, and the more aggressive cancers arise from luminal cells. Several haematopoietic malignancies seem to arise not from stem but from progenitor cells, even when essential precursor

genetic lesions are also present in the stem cells¹⁸. Finally, it is worth noting that many of these studies involve manipulation of a selected set of genetic pathways in a subset of cells of the target organ, which might reveal only a limited subset of the possible paths along which a malignancy may develop.

Carcinoma of the urinary bladder arises from the urothelium, a simple transitional epithelium lining the bladder lumen. This multi-layered epithelium consists of a luminal layer of fully differentiated umbrella cells that overlie intermediate cells with limited proliferative potential, and a basal layer of *Shh*-expressing cells. The *Shh*-expressing cells can form and propagate bladder-like organoids from single cells *in vitro*, and when genetically marked *in vivo* can be shown to replenish all other urothelial cells following injury, a regenerative activity that persists through multiple rounds of injury over long periods of time¹⁹. These properties identify *Shh*-expressing basal cells as probable urothelial stem cells.

The pro-carcinogen *N*-butyl-*N*-4-hydroxybutyl nitrosamine (BBN) is specifically activated in bladder and induces aggressive muscle-invasive bladder carcinoma over time with little effect on other tissues^{20,21}. Nitrosamines are potent mutagens present in cigarette smoke²², which is the most important known risk factor for human bladder cancer^{23,24}. Here, using BBN carcinogenesis and genetic tools

¹Institute for Stem Cell Biology and Regenerative Medicine, Stanford University School of Medicine, Stanford, California 94305, USA. ²Department of Developmental Biology, Stanford University School of Medicine, Stanford, California 94305, USA. ³Department of Pathology, Stanford University School of Medicine, Stanford, California 94305, USA. ⁴Stanford Immunology, Stanford University School of Medicine, Stanford, California 94305, USA. ⁵Department of Urology, Stanford University School of Medicine, Stanford, California 94305, USA. ⁶Department of Biochemistry, Stanford University School of Medicine, Stanford, California 94305, USA. ⁷Howard Hughes Medical Institute, Stanford University School of Medicine, Stanford, California 94305, USA.

⁸Correspondence should be addressed to K.S. or P.A.B. (e-mail: shink@ohsu.edu or pbeachy@stanford.edu)

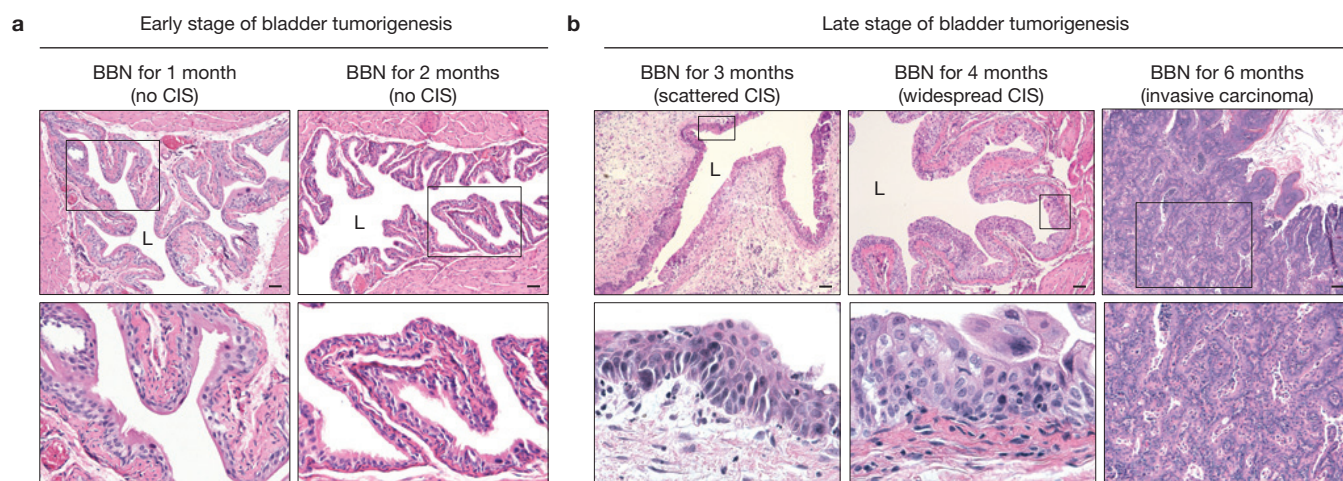


Figure 1 Histopathology of murine nitrosamine-induced bladder carcinoma mimics progression of human urothelial CIS to invasive carcinoma. (a,b) Histopathological analysis (haematoxylin and eosin (H&E) staining) of early (a) and late (b) stages of *N*-butyl-*N*-4-hydroxybutyl nitrosamine (BBN)-induced bladder carcinogenesis (see also Supplementary Table 1). The lower panels show magnified views of the outlined regions in the

upper panels. Note the appearance, beginning at 3 months of BBN exposure, of histologic abnormalities, including nuclear atypia, crowding, and architectural disarray histologically identical to human CIS, and leading to invasive carcinoma by 6 months of BBN exposure. L, bladder lumen. Scale bars, 50 μ m. Repeated experimental results are shown in Supplementary Table 1.

to mark or ablate cells, we demonstrate that *Shh*-expressing basal stem cells of the urothelium are the cell of origin for murine invasive urothelial carcinoma. Using multi-colour cell marking and lineage tracing, we also show that precursor lesions during progression to invasive carcinoma arise from aggressive clonal expansion of single urothelial cells whose progeny colonize a major portion of the urothelium to generate a carcinoma *in situ* (CIS) precursor lesion. Finally, although *Shh*-expressing cells within this lesion become tumour-initiating cells, *Shh* expression is lost by the time carcinomas develop, demonstrating that the phenotypic properties of mature tumour cells can diverge from those of the cancer cell of origin.

RESULTS

Similarity of human and BBN-induced mouse bladder cancer

We examined mouse bladder tissues after exposure to BBN in drinking water and noted that the histopathology of BBN-exposed bladders in our murine model evolves in a manner similar to human muscle-invasive carcinoma^{21,25}. Bladder tissues thus appear normal, without cellular changes or tissue disorganization within the first 2 months of BBN exposure (Fig. 1a and Supplementary Table 1). Histologic abnormalities appeared at 3 months of BBN exposure, including areas of nuclear atypia, crowding, and architectural disarray histologically indistinguishable from human CIS (Fig. 1b and Supplementary Table 1). At 4 months of BBN exposure, CIS became robust and widespread in most animals, with extensive urothelial thickening (Fig. 1b and Supplementary Table 1), and muscle-invasive carcinoma invariably developed by 6 months of BBN exposure (Fig. 1b and Supplementary Fig. 1), with consequent illness and morbidity necessitating euthanasia by 8 months of BBN exposure. The urothelial thickening caused by BBN exposure is distinct from hyperplasia that is rapidly induced by bacterial or chemical injury¹⁹, as it requires months of BBN exposure to arise, does not recede, and is associated with CIS (Supplementary Fig. 2).

CIS and invasive carcinoma develop from *Shh*-expressing basal stem cells

The presence of basal cell character in tumour-propagating cells^{26,27} is consistent with our observation that the basal cell marker CK5 is expressed throughout BBN-induced tumours (see below). As other cancers with basal character derive from luminal cells^{11,12}, we examined the cancer cell of origin by prospective marking of basal urothelial stem cells. We injected *Shh*^{CreER}; *R26*^{mTmG} mice with tamoxifen (TM) to activate CreER and induce excision of mT (membrane-targeted tdTomato) and permanent marking of *Shh*-expressing basal cells and their progeny by expression of mG (membrane-targeted enhanced green fluorescent protein (EGFP)). TM treatment was followed by 4- and 6-month courses of exposure to BBN (Fig. 2 and Supplementary Fig. 3). We noted mG marking of both the CIS lesion at 4 months (5/5 mice) and invasive carcinomas at 6 months (6/6 mice; Fig. 2a,b and Supplementary Fig. 3a,b), indicating that both derive from *Shh*-expressing basal stem cells and that CIS may represent a precursor lesion in muscle-invasive carcinoma development, as widely believed in human patients²⁵. Importantly, no unmarked invasive carcinomas were observed, despite the presence of many unmarked supra-basal and luminal cells at the beginning of BBN exposure, suggesting that invasive carcinoma is exclusively derived from *Shh*-expressing basal stem cells.

Ablation of basal stem cells abrogates BBN carcinogenesis

We explicitly tested the requirement for basal stem cells in tumour formation by injecting TM into mice of the genotype *Shh*^{CreER}; *R26*^{DTA}, in which expression of an attenuated form of the diphtheria toxin fragment A (DTA; refs 28–30) results in highly efficient ablation of *Shh*-expressing basal cells and consequent loss of high levels of CK5 expression. The low levels of CK5 in remaining cells resemble those normally seen in intermediate cells (Fig. 3a), which do not express *Shh*. These mice failed to maintain normal bladder epithelial architecture

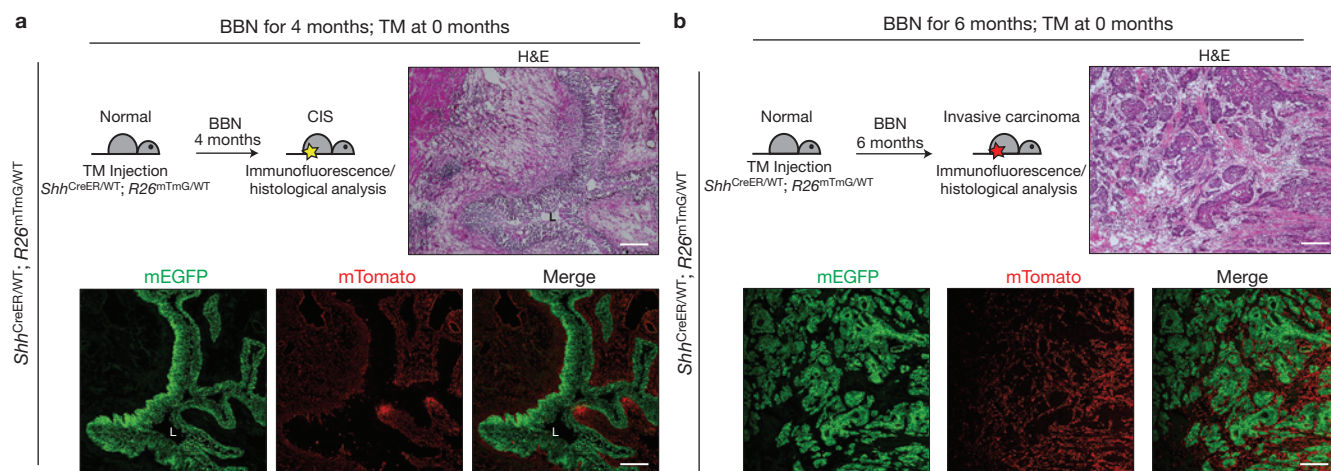


Figure 2 *Shh* expression marks basal stem cells that give rise to CIS and invasive bladder carcinoma. **(a,b)** Schematic diagrams (top left) show the experimental strategies for marking *Shh*-expressing cells and their progeny before BBN induction of CIS **(a)** or invasive carcinoma **(b)**. *Shh*^{CreER}; *R26*^{mTmG} mice injected with tamoxifen (TM) on 3 consecutive days were treated with BBN for 4 months to induce CIS lesions **(a)** or 6 months to induce invasive carcinoma **(b)**, followed by histological

analysis (H&E) or analysis of mG/mT expression. All tumours and CIS lesions are marked by expression of mG, indicating that invasive carcinoma and CIS originate from *Shh*-expressing basal cells, not intermediate or luminal cells. L, bladder lumen; mG, membrane-targeted enhanced green fluorescent protein (EGFP); mT, membrane-targeted tdTomato. Repeated experimental results are shown in Supplementary Fig. 3. Scale bars, 50 μ m.

(Fig. 3b) and died within 8–10 months, consistent with previous findings on urothelial turnover³¹ and the role of basal urothelial stem cells in bladder homeostasis¹⁹.

On exposure to BBN we found that vehicle-injected control mice developed invasive carcinoma marked by high-level expression of CK5 (7 of 7 mice, Fig. 3c and Supplementary Fig. 4), whereas TM-injected mice, in which basal stem cells were ablated, did not develop invasive carcinoma (0 of 7 mice, Fig. 3c), even when BBN exposure continued for 8 months (Supplementary Fig. 4). Basal stem cells thus are absolutely required for formation of BBN-induced tumours, and the more differentiated supra-basal and luminal cells that remain in these TM-injected animals are not susceptible to BBN-induced carcinogenesis. The finding that BBN-induced carcinomas are comprised entirely of the progeny of marked basal stem cells without contribution from unmarked intermediate or luminal cells, together with the failure of BBN to induce tumours within animals lacking basal stem cells, constitutes strong evidence that invasive bladder carcinoma originates exclusively from the *Shh*-expressing basal urothelial stem cell.

Although TM-injected *Shh*^{CreER}; *R26*^{DTA} animals exposed to BBN for 6 months exhibited disrupted epithelial architecture (Fig. 3c), epithelial integrity was preserved after 3 or 4 months of BBN exposure, with only mild urothelial thickening (Fig. 3d). The residual levels of CK5 expression were similar to those of normal intermediate urothelial cells (Fig. 3a), suggesting that the limited urothelial thickening induced by BBN exposure may be supported by proliferation of intermediate cells. Progressive deterioration of urothelial integrity over longer periods of time in animals lacking basal stem cells, with or without carcinogen treatment, suggests the exhaustion of limited proliferative capacity of these intermediate cells.

To determine how loss of basal stem cells affects CIS during tumorigenesis of BBN-induced invasive cancer, histopathology of

TM-injected *Shh*^{CreER}; *R26*^{DTA} animals was evaluated at monthly intervals during BBN exposure. These animals developed CIS lesions to a significantly reduced extent (Fig. 4a,b and Supplementary Tables 2 and 3). Epithelial architecture in basal cell-ablated bladders was maintained after 3 or 4 months of BBN exposure, with normal expression of the luminal marker CK18 (Fig. 4c,d). The low frequency of CIS and absence of tumours at later stages of BBN exposure (Fig. 3c) in these mice thus are not due to gross disruption of urothelial architecture, and these results together strongly suggest that *Shh*-expressing basal cells are a cell of origin for invasive carcinomas and for precursor lesions during bladder tumorigenesis.

***Shh*-positive cells in the intermediate lesion as a cell of origin of tumour-propagating cells**

To analyse the expression of *Shh* during tumour progression, *Shh*^{CreER}; *R26*^{mTmG} mice were exposed to BBN for 4 months to generate CIS lesions, then injected with TM to label *Shh*-expressing cells a few days before euthanization (Fig. 5a, upper left). We found that although all cells in CIS lesions of these mice expressed CK5 at a high level (Fig. 5a and Supplementary Fig. 5a), only a basal subset of these CK5-positive cells expressed mG, indicating maintenance of *Shh* expression in a basal subpopulation of CK5-positive cells (Fig. 5a and Supplementary Fig. 5a). Other more luminal progeny of these basal cells lack *Shh* expression but retain high levels of CK5.

To investigate the cancer-forming capacities of these two CIS cell populations, *Shh*^{CreER}; *R26*^{mTmG} mice previously exposed to BBN for 4 months were injected with TM, thus marking *Shh*-positive cells in the basal layer, whereas the remaining cells retain expression of mT. These mice were then subjected to further exposure to BBN for 2 months (Fig. 5b). These mice developed aggressive bladder cancers (Fig. 5c, left panel) comprising both mG-positive and mT-positive cells (Fig. 5c, right panel), thus indicating that both *Shh*-positive and *Shh*-negative CIS cells contribute to invasive bladder cancers.

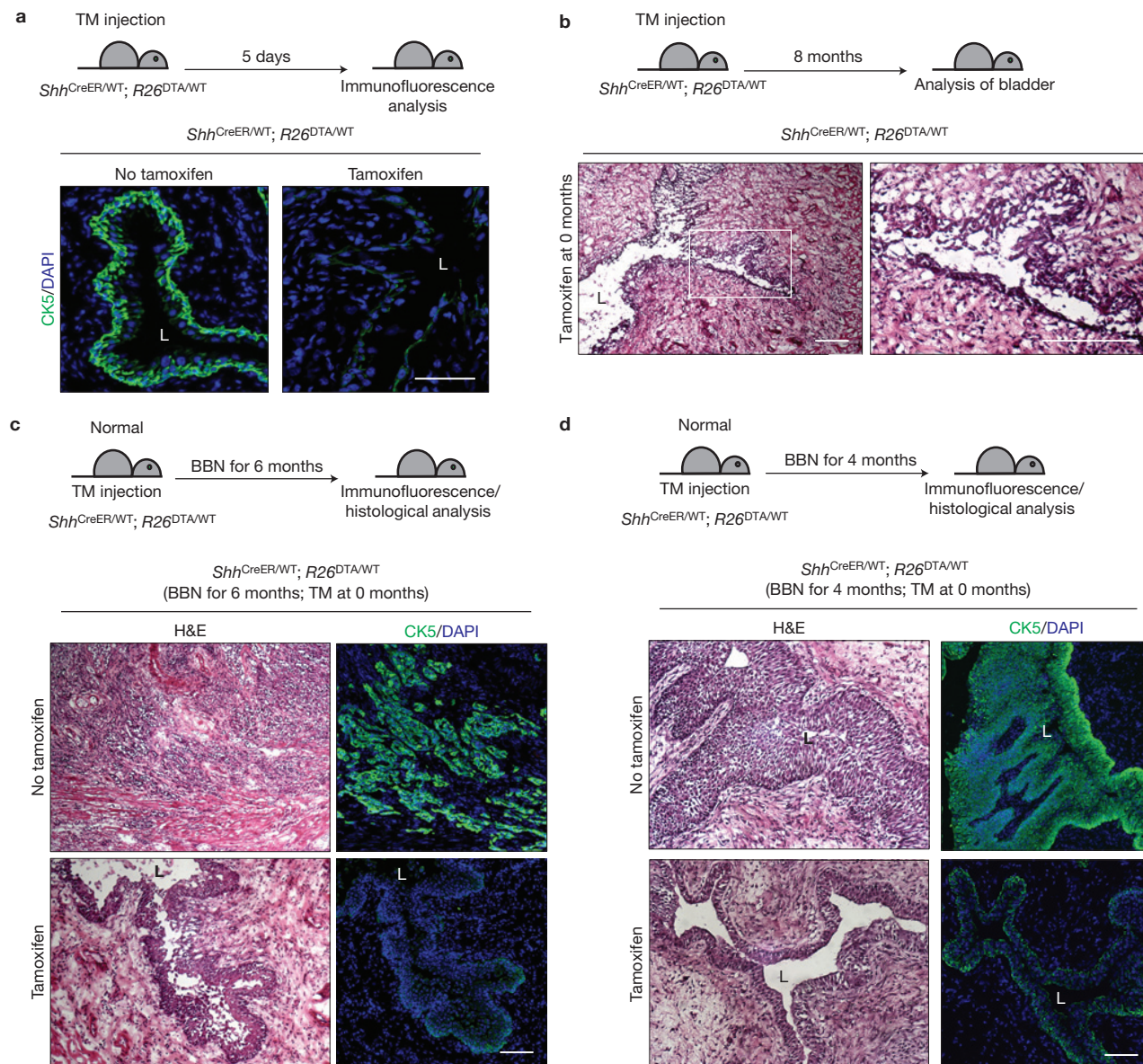


Figure 3 Ablation of *Shh*-expressing basal stem cells confers resistance to nitrosamine-induced formation of invasive bladder carcinoma. **(a)** TM was injected into *Shh*^{CreER}; *R26*^{DTA} mice on 5 consecutive days. Five days after the last TM injection, bladders were analysed by immunostaining. Sections from the bladders of control vehicle-injected or TM-injected mice (left and right panels, respectively) were stained for CK5 (green). Note that TM treatment effectively ablates basal epithelial cells in the *Shh*^{CreER}; *R26*^{DTA} mouse bladder. **(b)** *Shh*^{CreER}; *R26*^{DTA} mice were injected with TM on 5 consecutive days to ablate *Shh*-expressing basal cells and were maintained for 8 months without BBN exposure. Histology of the bladder from a mouse

8 months after TM injection shows the failure of maintenance of normal bladder epithelium, resulting from loss of stem cells. The right panel shows an enlarged view of the outlined region in the left panel. **(c,d)** TM was injected into *Shh*^{CreER}; *R26*^{DTA} mice on 5 consecutive days to ablate *Shh*-expressing basal cells, and mice were exposed to BBN for 6 **(c)** or 4 **(d)** months. Bladder tissues were analysed by H&E staining (left panels) and immunostaining for CK5 (green, right panels). The upper panels show bladders from vehicle controls (no TM). L, bladder lumen. Repeated experimental results for **c** are shown in Supplementary Fig. 4. Scale bars, 50 μ m.

We established transplant models in which cells from primary BBN-induced bladder tumours were injected into immunocompromised mice to give rise to a secondary tumour, either orthotopically into the intramural portion of the bladder dome (Supplementary Fig. 5c) or subcutaneously into the flank. We then used these transplant models to test genetically marked cells from *Shh*^{CreER}; *R26*^{mTmG} animals treated with TM at 4 months, followed by exposure to BBN for an additional 2 months as described above (Fig. 5b). EpCAM⁺ cells (expressed in tumour cells, not in stroma) marked by

expression of mG⁺ or mT⁺ were separated by fluorescence-activated cell sorting (FACS; Supplementary Fig. 5b) and transplanted orthotopically at three dilutions to test their tumour-propagating abilities (Fig. 5d). We found that mG⁺ cancer cells at all three dilutions were able to give rise to secondary tumours, whereas mT⁺ cells did not (Fig. 5e and Supplementary Fig. 5d). Similar results were noted when cancer cells were separated by using only mG or mT expression in the subcutaneous model (Supplementary Fig. 6). We conclude that *Shh*-expressing cells in the CIS lesions generate

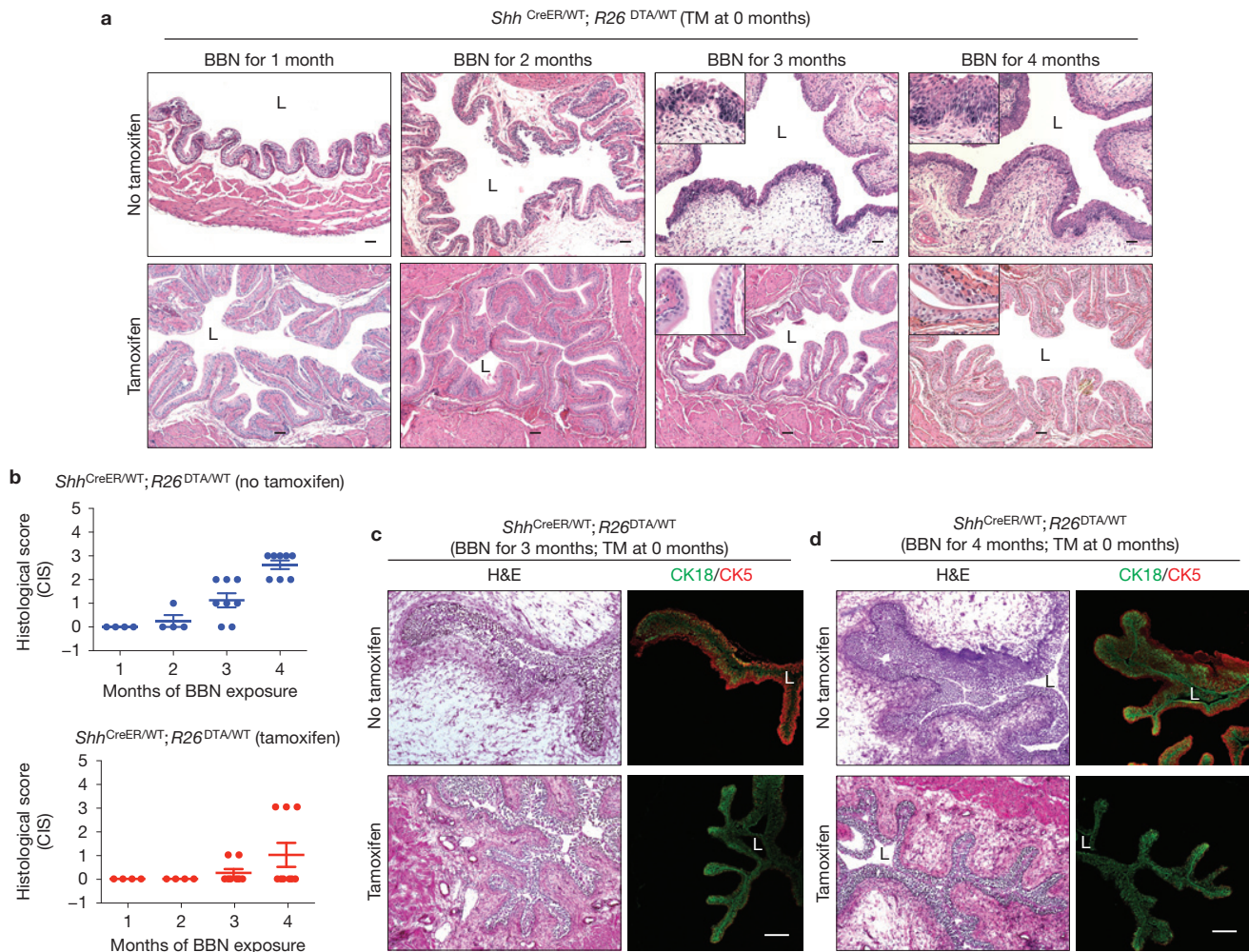


Figure 4 Ablation of *Shh*-expressing basal stem cells reduces CIS during nitrosamine-induced carcinogenesis while preserving urothelial architecture. **(a)** Histopathological analysis (H&E) of TM-injected *Shh^{CreER}; R26^{DTA}* mice after 1–4 months of BBN exposure. Repeated experimental results are shown in Supplementary Tables 2 and 3. **(b)** Histopathological evaluation of CIS in bladders from *Shh^{CreER}; R26^{DTA}* mice (Supplementary Tables 2 and 3). Scores from 0 to 3 are based on the extent of CIS within urothelium (0, none; 1, <10%; 2, 10–30%; 3, >30%). No invasive carcinoma and little or no CIS was induced by BBN exposure in animals with ablated stem cells. $n=4$ (1 month), $n=4$ (2 months), $n=8$ (3 months), $n=8$ (4 months) for

vehicle-treated *Shh^{CreER}; R26^{DTA}* mice; $n=4$ (1 month), $n=4$ (2 months), $n=8$ (3 months), $n=9$ (4 months) for TM-treated *Shh^{CreER}; R26^{DTA}* mice. Data are presented as mean \pm s.e.m. **(c, d)** *Shh^{CreER}; R26^{DTA}* mice were injected with TM on 5 consecutive days to ablate *Shh*-expressing basal cells and exposed to BBN for 3 **(c)** and 4 **(d)** months. Sections from the bladders of control vehicle-injected or TM-injected mice (top and bottom panels, respectively) were stained for the luminal and basal markers, CK18 and CK5 (green and red, respectively). Note that luminal cells are well preserved at intermediate stages of BBN exposure in stem-cell-ablated animals. L, bladder lumen. Scale bars, 50 μ m.

the carcinoma cells that are capable of propagating the tumour in transplantation experiments.

Absence of *Shh* expression in invasive carcinoma

In our BBN murine model invasive carcinomas arise from *Shh*-expressing basal stem cells, with tumour development progressing through basal cells of the intermediate CIS lesion. As previous analyses revealed very low or undetectable expression of *SHH* messenger RNA in a group of human bladder carcinoma samples³², we further investigated *Shh* expression by inducing invasive carcinomas with 6 months of BBN exposure in *Shh^{CreER}; R26^{mTmG}* mice, then injecting with TM a few days before euthanization (Fig. 6a). We found that invasive carcinomas were entirely devoid of mG (Fig. 6b), which should provide a reliable indication of *Shh* expression¹⁹, despite continued strong expression of CK5. We further confirmed that

expression of *Shh* is lost on progression to invasive carcinoma by quantitative PCR with reverse transcription from material obtained by laser capture microdissection from BBN-induced bladder tumours (Fig. 6c,d and Supplementary Fig. 7). Thus, although *Shh* expression marks the basal cell of origin for invasive carcinomas and persists in the precursor lesion for these tumours, it is completely absent in the fully formed tumour. Our results with BBN-induced invasive bladder carcinoma mirror those reported for a set of human transitional cell carcinoma samples³², most of which were invasive³³.

Lineage and clonality in BBN-induced bladder carcinoma

The development of recurrent, multifocal tumours is a common characteristic of human urothelial carcinoma, with some studies concluding that such tumours are clonally related, whereas others argue for distinct cellular origins^{34–43}. To investigate lineage

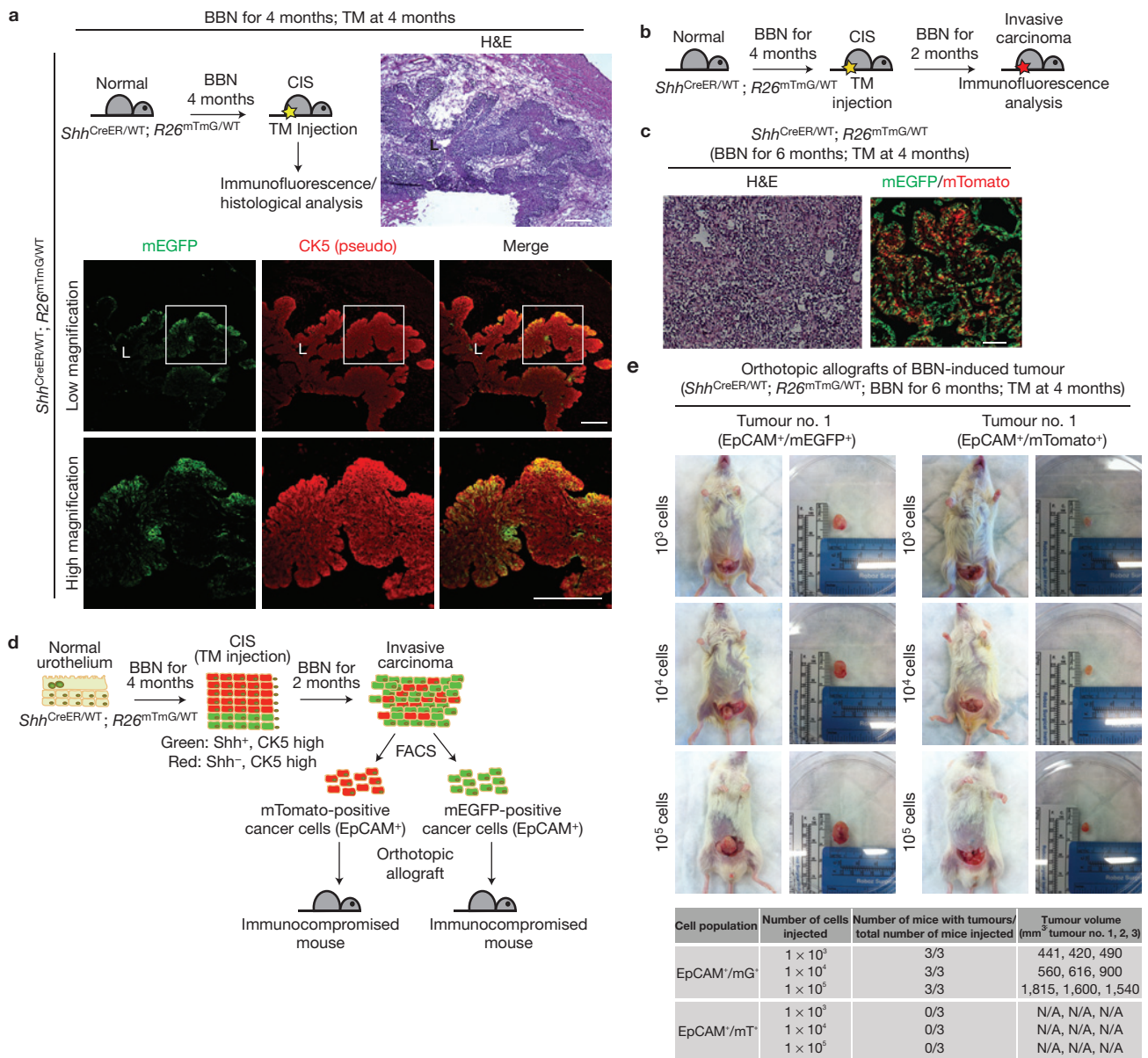


Figure 5 *Shh*-positive and -negative cells in the CIS lesion contribute to invasive carcinoma, but tumour-propagating cells derive exclusively from *Shh*-positive cells. **(a)** Experimental scheme (top left panel) to label *Shh*-expressing cells in the CIS lesion. Following 4 months of BBN exposure to induce CIS, $Shh^{CreER/WT}; R26^{mTmG/WT}$ mice were injected with TM on 3 consecutive days to label *Shh*-expressing cells before euthanization. Bladder tissues were analysed by H&E staining (top right panel) or by immunostaining for mG and CK5 (green and red, respectively). The lower panels show magnified views of the regions highlighted by white squares in the panels immediately above. **(b)** Experimental scheme for marking *Shh*-positive and -negative cells in CIS lesions, and to track them into carcinoma formation. **(c)** $Shh^{CreER/WT}; R26^{mTmG/WT}$ mice exposed to BBN for 4 months and injected with TM on 3 consecutive days were subsequently exposed to BBN for 2 more months. Invasive carcinomas from these

animals were analysed by H&E staining (left panel) or for expression of mG or mT, which respectively marks cells that expressed (green) or did not express (red) *Shh* at the time of TM injection. **(d)** Experimental scheme to determine the tumour-propagating ability of carcinoma cells. mG/EpCAM-positive and mT/EpCAM-positive cells from invasive carcinomas generated as described in **b** were isolated by FACS and transplanted intramurally into the dome of the bladder. **(e)** Orthotopic transplantation with serial dilutions of mG/EpCAM-positive and mT/EpCAM-positive cells from a single tumour. Results of transplantations from three different tumours, summarized below, show that only *Shh*-expressing cells in the CIS lesion will subsequently become tumour-propagating cells in transplantation experiments. L, bladder lumen. Repeated experimental results for **a** and **e** are shown in Supplementary Fig. 5a,d, respectively. Scale bars, 50 μ m.

relationships and tissue dynamics in our model we used multi-colour marking before BBN-induced carcinogenesis. The 'Rainbow' mouse^{44–46} ($R26^{Rainbow}$; Fig. 7a) initially expresses EGFP but can recombine in a Cre-dependent fashion to express any of three additional distinct fluorescent proteins. Individual cells in the bladders of

$Actin^{CreER}; R26^{Rainbow}$ mice treated with an appropriate level of TM thus are stochastically labelled in approximately equal numbers by permanent and heritable expression of one of four distinct fluorescent proteins (Fig. 7a,b and Supplementary Fig. 8). On exposure to BBN, these animals developed large CIS lesions marked by a single colour

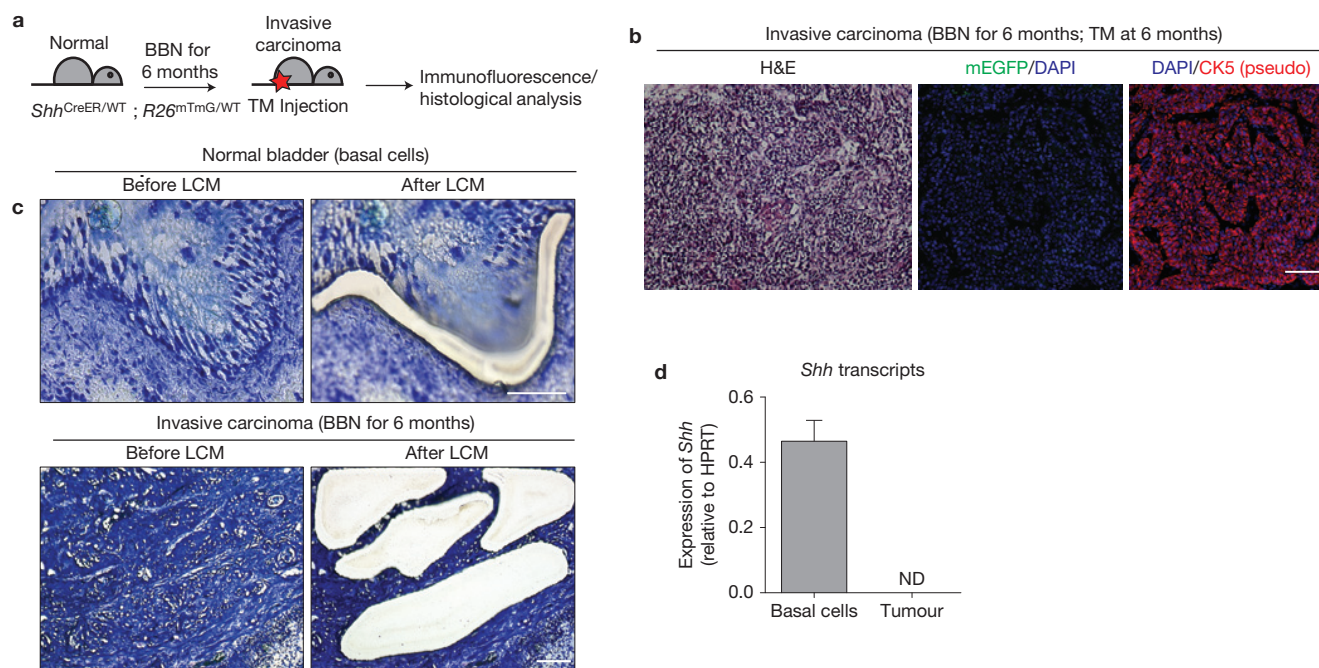


Figure 6 *Shh* expression is lost in invasive carcinoma of murine bladder. (a) Experimental scheme for marking of *Shh*-expressing cells in invasive carcinoma induced by 6 months of BBN exposure. (b) *Shh*^{CreER}; *R26*^{mTmG} mice exposed to BBN for 6 months were injected with TM on 3 consecutive days to label *Shh*-expressing cells before euthanization, and the bladder carcinoma was analysed by H&E staining (left panel) or by immunostaining for mG and CK5 (green and red, respectively, in middle and right panels), with DAPI staining to visualize nuclei. Note the lack of mG expression in the carcinoma, indicating the absence of *Shh* expression, whereas CK5 expression is seen in all cancer cells. (c) Laser capture microdissection (LCM) of normal basal

cell layer (upper panels) in untreated bladder and of carcinoma cells within tumour (lower panels). Nine tumour areas were assessed (3 different tumour areas from 3 distinct tumours) and representative images are shown here (area no. 1 from tumour no. 1). Other areas from 3 distinct tumours (area nos 2–3 in tumour no. 1; area nos 1–3 for tumour no. 2; area nos 1–3 from tumour no. 3) are shown in Supplementary Fig. 7a. (d) *Shh* mRNA is detected in cells microdissected from normal basal cells but absent from carcinoma cells. ND, not detected. Data are presented as mean \pm s.e.m. from 3 technical replicates; 9 tumour areas were assessed (3 different tumour areas from 3 distinct tumours). Scale bars, 50 μ m.

and spanning extensive regions of contiguous cells (Fig. 7c, CIS no. 1). The entire urothelium thus consists of the progeny of one (monoclonal) or at most a few cells (oligoclonal; Fig. 7c, CIS no. 2).

On further BBN exposure we observed that invasive carcinomas seem to arise clonally, with a large tumour of a single colour occupying the entire bladder (monoclonal; Fig. 7d) or with a few discrete tumour foci that are each labelled with a single colour (oligoclonal; Fig. 7e). Oligoclonal tumours are usually accompanied by nearby CIS regions of the same colour (Fig. 7e) and such clonally related CIS regions can be easily identified when the tumour is less advanced. Thus, at 5 months of BBN exposure we observed two distinctly marked CIS lesions together occupying the entire urothelium, with a small carcinoma beginning to develop entirely within one of these two distinctly marked CIS lesions (Fig. 7c, CIS no. 2). Taken together, our observations suggest that CIS lesions develop clonally from one or a few cells with the remarkable ability to aggressively spread and displace other urothelial cells within major contiguous portions of the urothelium.

DISCUSSION

Nitrosamines are powerful mutagens found in cigarette smoke, which is the most important known risk factor for human bladder cancer^{22–24}. Our use of the bladder-specific carcinogen BBN in the mouse thus mimics human bladder carcinogenesis in the type of carcinogen employed, in the lack of any prior bias regarding cell type or genetic

pathway, and in carcinogen exposure over an extended period of time, thus permitting incremental progression and cell selection through genetic and tissue changes.

The previous identification of *Shh*-expressing basal cells as urothelial stem cells was based in part on *in vivo* genetic marking¹⁹. Our use in this work of chemical carcinogenesis rather than genetic methods to induce urothelial carcinoma was a critical factor in permitting use of the same genetic methods to mark *Shh*-expressing basal stem cells and show that they give rise to invasive urothelial carcinomas. Our findings exclude other urothelial cells as the cell of origin because marking of *Shh*-expressing basal cells exclusively generates marked tumours and because ablation of these cells renders the bladder incapable of generating a tumour. Although it is conceivable that tumours from supra-basal cells could be marked if basal cells generate other urothelial cell types during BBN exposure, we should also then see some unmarked tumours, as many unmarked supra-basal cells are also present in the urothelium at the time of BBN exposure. Furthermore, conversion of basal cells to supra-basal cells is a low-frequency event, as we see very little proliferation and urothelial turnover within the first months of BBN exposure (Supplementary Fig. 2). Similarly, if tumours could arise from supra-basal cells, we would expect to see tumours arising in the experiment that ablates *Shh*-expressing cells, as the urothelium appears normal with respect to its basic architecture and retains intermediate cells and well-differentiated umbrella cells. The fundamental integrity of

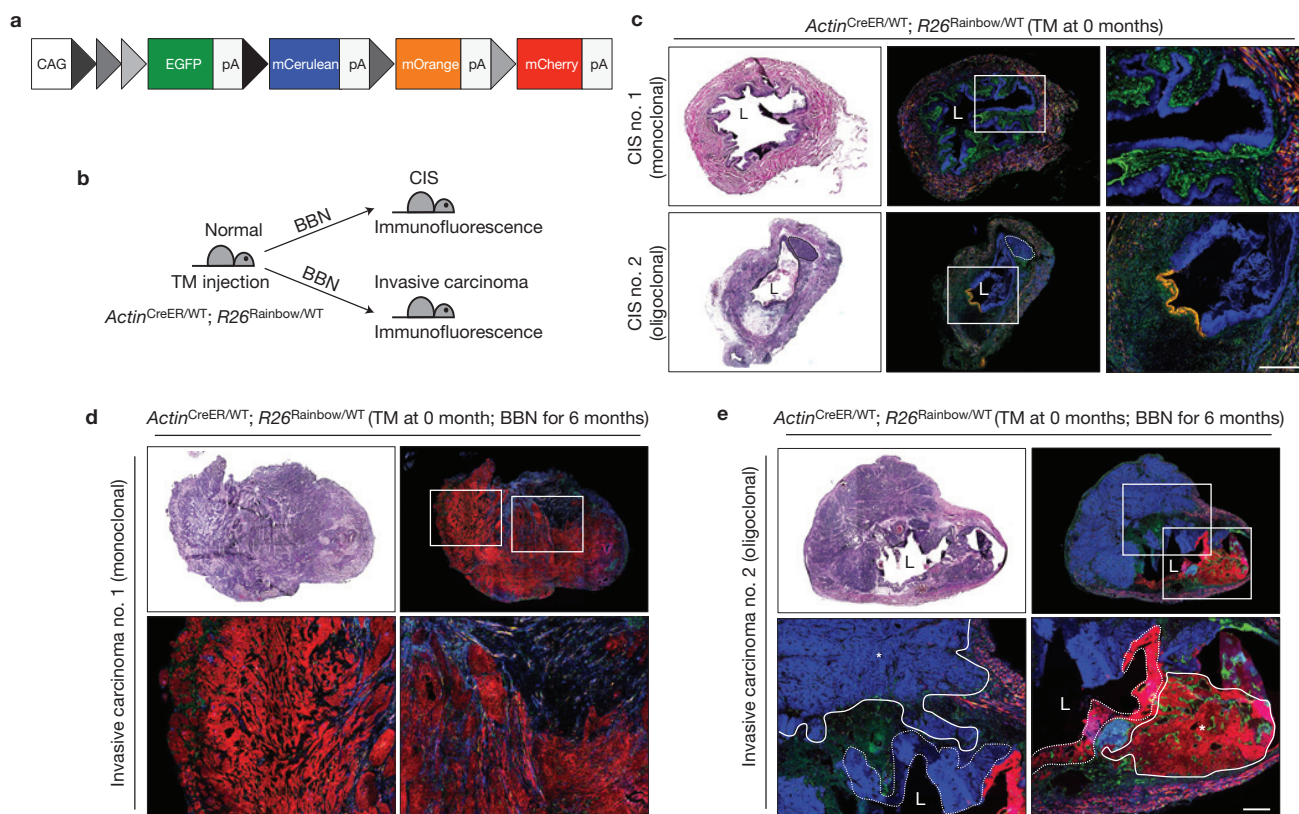


Figure 7 Four-colour marking reveals monoclonal and oligoclonal urothelial colonization and carcinoma formation on nitrosamine exposure. (a) Schematic diagram of the Rainbow allele. By virtue of three different lox sites (lox2272, loxN and loxP), individual cells express either EGFP (before Cre-mediated recombination) or mCerulean, mOrange or mCherry (after Cre-mediated recombination). (b) Experimental scheme to investigate clonal relationships during bladder carcinogenesis. A low dose of TM injected into *Actin^{CreER}; R26^{Rainbow}* mice stochastically labelled bladder cells with one of four fluorescence colours, and these animals then were exposed to BBN until they developed CIS (c) or invasive carcinoma (d,e). (c) Bladders from TM-injected *Actin^{CreER}; R26^{Rainbow}* mice exposed to BBN for 4 months (CIS no. 1) or 5 months (CIS no. 2) and analysed by H&E staining (left panels) or for

four-colour fluorescence. The right panels show magnified views of the regions highlighted by white rectangles in the middle panels. CIS lesions covering the entire urothelium arise from a single (no. 1, monoclonal) or two cells (no. 2, oligoclonal). A small carcinoma arising within the blue-marked CIS no. 2 is outlined by a dotted line. (d,e) Bladders from TM-injected *Actin^{CreER}; R26^{Rainbow}* mice exposed to BBN for 6 months were analysed by H&E staining (top left panels) or for four-colour fluorescence (top right panels). The bottom panels show magnified views of the regions highlighted by white rectangles in the top right panels. Carcinomas within a single bladder arise from one (d, monoclonal) or several (e, oligoclonal) cells, respectively. In e, tumours are outlined by solid lines with asterisks and nearby CIS regions are outlined by dotted lines. L, bladder lumen. Scale bars, 50 μ m.

the urothelium in these animals is suggested by their survival for at least 8 months after the ablation of stem cells, and is consistent with the previous assessment of a 10-month turnover time for murine urothelium³¹. The exclusive presence of marked tumours in the marking experiment and the absence of tumours in the ablation experiment together constitute strong positive and negative evidence that clearly identifies the *Shh*-expressing basal urothelial stem cell as the exclusive cell of origin in invasive bladder carcinoma.

As recently demonstrated, tumour-propagating cells isolated from human bladder carcinomas have basal character^{26,27}, and thus resemble the basal cell of origin identified here. This relationship, however, is distinct from that in tumours such as mammary adenocarcinoma, in which a tumour with basal character arises from a luminal cell of origin^{11,12}, or prostate adenocarcinoma, which has luminal character but evidently can originate from luminal or basal cells^{13–17}. In addition, despite the apparent basal character of tumour-propagating cells of bladder carcinoma, most human invasive bladder carcinomas and the invasive carcinoma cells of our murine model differ strikingly from their cells of origin in having lost expression of *Shh*.

In human bladder carcinogenesis, CIS is widely thought of as a precursor to invasive carcinoma²⁵. Such lesions have long been thought of as stages in the development of other cancers, as well. For example, prostatic intraepithelial neoplasia in prostate adenocarcinoma^{47,48}, pancreatic intraepithelial neoplasia in pancreatic adenocarcinoma^{49,50}, mammary ductal CIS (ref. 51), and adenomatous polyps of the colon⁵² are commonly discussed as intermediate stages of cancer progression, and these lesions often carry genetic alterations similar to those of fully developed carcinomas. Conclusive evidence tracing the origin of malignancy directly to such precursor lesions, however, has largely been lacking. The tools of lineage tracing applied here in the murine BBN model allow us to definitively address the relationship of intermediate lesions to invasive carcinoma, and we have been able to confirm not only that CIS is within the lineage leading to invasive carcinoma, but also to identify basal *Shh*-expressing cells within the CIS lesion as the cells that acquire tumour-propagating ability on formation of an invasive carcinoma.

One of the most striking findings to emerge from our multi-colour lineage studies in the BBN model is the remarkable ability of a single

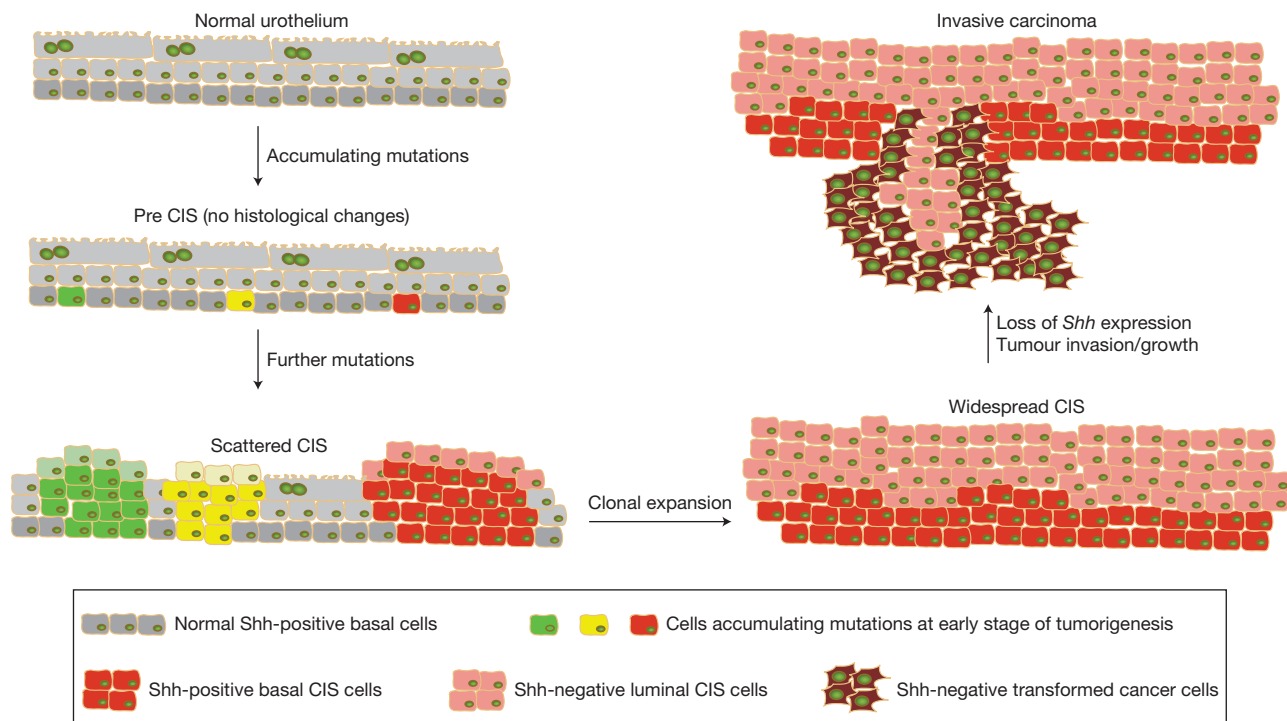


Figure 8 Model for progression of nitrosamine-induced bladder carcinogenesis. BBN-induced invasive carcinoma of the mouse bladder arises from basal stem cells that express *Shh* and CK5. Normal basal cells accumulate mutations at early stages of carcinogenesis and initiate clonal expansions to form intermediate CIS lesions, as indicated by

green, yellow and red colours. During this process, one or two clones become dominant and expand to repopulate the entire urothelium, generating mono/oligo-clonal CIS lesions. CIS basal cells in one of these lesions then lose expression of *Shh* on establishment of invasive carcinoma.

urothelial cell to sweep through and displace all other cells within a large contiguous portion of the urothelium. This finding is probably relevant to the extensive literature on clonal relationships among synchronous or metachronous human bladder tumours^{34–43}. The tools that previously have been used to determine clonal relationships include X-inactivation analysis, comparative genome hybridization, loss of heterozygosity analyses, and mutational analysis to compare chromosomal and genetic alterations in different tumours. The conclusions of these studies vary, and it has been proposed that multifocal tumours with a monoclonal origin may have divergent late genetic changes whose analysis could lead to the erroneous conclusion that they are multiclonal^{53,54}. The uncertainty in interpreting these types of results thus arises in part from uncertainty regarding the sequence of genetic events within tumours that are used as the basis for analysis. Our multi-colour marking experiments in the BBN model use distinctive marks generated before carcinogenesis and thus remove all ambiguity with regard to sequence. Our observation that a single marked cell under mutagenic pressure can aggressively proliferate and spread through extensive contiguous regions of the urothelium provides a clear basis for the clonal relationships identified among multifocal tumours within a single bladder^{34–38}. This aggressive intraepithelial expansion of a single clone and our observations of invasive tumours surrounded by non-invasive regions of clonally related CIS urothelium also provide a correlate for the commonly reported occurrence of a tumour surrounded by a region of abnormal but benign epithelium^{55–57}. Finally, the occurrence of two or three unrelated CIS lesions or tumours within a single bladder illustrates

the possibility of generating multifocal tumours of distinct clonal origin; the probability of this occurrence may depend on the degree of mutagenic pressure.

The events of carcinoma initiation and progression are summarized in Fig. 8, and begin with accumulation of mutations in *Shh*-expressing urothelial basal stem cells, the cancer cell of origin. These mutations allow the progeny of a single cell to sweep through and colonize an extensive portion of the urothelium and form a CIS precursor lesion. Within this lesion, *Shh*-positive basal cells accumulate further mutations, leading to further clonal expansion and ultimately to transformation and invasion of the stromal and muscle layers of the bladder. The latter stages of this process are consistently accompanied by loss or attenuation of *Shh* expression, and further studies will be required to establish the significance of this loss. One of the key features of our findings is that progression to invasion occurs in the context of a precursor lesion with pre-neoplastic changes that aggressively spreads through most if not all of the urothelium. Resection of invasive carcinomas, even if complete, thus may leave in place urothelial cells that already have taken several early steps along the path to invasive tumour formation, thus potentially accounting for the frequent recurrence and high morbidity of invasive human bladder cancer. □

METHODS

Methods and any associated references are available in the [online version of the paper](#).

Note: Supplementary Information is available in the online version of the paper

ACKNOWLEDGEMENTS

We thank I. Weissman and Y. Rinkevich for their generous provision of the Rainbow mouse, T. Desai, A. Oro and J. Sage for their critical reading of the manuscript, and the Stanford Neuroscience Microscopy Service for help with confocal microscopy. This research was supported in part by grants from the National Institutes of Health (P.A.B.) and a Pathway to Independence Award (K99/R00) to K.S. P.A.B. is an investigator of the Howard Hughes Medical Institute.

AUTHOR CONTRIBUTIONS

K.S. and P.A.B. conceived ideas and experimental design. K.S. and A.L. performed the experiments. J.I.O. performed the histopathological analysis, J.D.H. aided in orthotopic injection, S.K. performed the genotyping of experimental mice, and M.H.H. helped analyse data. K.S. and P.A.B. wrote the manuscript.

COMPETING FINANCIAL INTERESTS

The authors declare no competing financial interests.

Published online at www.nature.com/doi/10.1038/ncb2956

Reprints and permissions information is available online at www.nature.com/reprints

- Reya, T., Morrison, S. J., Clarke, M. F. & Weissman, I. L. Stem cells, cancer, and cancer stem cells. *Nature* **414**, 105–111 (2001).
- Taipale, J. & Beachy, P. A. The Hedgehog and Wnt signalling pathways in cancer. *Nature* **411**, 349–354 (2001).
- Bonnet, D. & Dick, J. E. Human acute myeloid leukemia is organized as a hierarchy that originates from a primitive hematopoietic cell. *Nature Med.* **3**, 730–737 (1997).
- Al-Hajj, M., Wicha, M. S., Benito-Hernandez, A., Morrison, S. J. & Clarke, M. F. Prospective identification of tumorigenic breast cancer cells. *Proc. Natl Acad. Sci. USA* **100**, 3983–3988 (2003).
- Blanpain, C. Tracing the cellular origin of cancer. *Nat. Cell Biol.* **15**, 126–134 (2013).
- Barker, N. *et al.* Crypt stem cells as the cells-of-origin of intestinal cancer. *Nature* **457**, 608–611 (2009).
- Schepers, A. G. *et al.* Lineage tracing reveals Lgr5+ stem cell activity in mouse intestinal adenomas. *Science* **337**, 730–735 (2012).
- Flesken-Nikitin, A. *et al.* Ovarian surface epithelium at the junction area contains a cancer-prone stem cell niche. *Nature* **495**, 241–245 (2013).
- Chen, J. *et al.* A restricted cell population propagates glioblastoma growth after chemotherapy. *Nature* **488**, 522–526 (2012).
- Driessens, G., Beck, B., Caauwe, A., Simons, B. D. & Blanpain, C. Defining the mode of tumour growth by clonal analysis. *Nature* **488**, 527–530 (2012).
- Molyneux, G. *et al.* BRCA1 basal-like breast cancers originate from luminal epithelial progenitors and not from basal stem cells. *Cell Stem Cell* **7**, 403–417 (2010).
- Lim, E. *et al.* Aberrant luminal progenitors as the candidate target population for basal tumor development in BRCA1 mutation carriers. *Nat. Med.* **15**, 907–913 (2009).
- Lawson, D. A. *et al.* Basal epithelial stem cells are efficient targets for prostate cancer initiation. *Proc. Natl Acad. Sci. USA* **107**, 2610–2615 (2010).
- Mulholland, D. J. *et al.* Lin-Sca-1+CD49^{high} stem/progenitors are tumor-initiating cells in the Pten-null prostate cancer model. *Cancer Res.* **69**, 8555–8562 (2009).
- Goldstein, A. S., Huang, J., Guo, C., Garraway, I. P. & Witte, O. N. Identification of a cell of origin for human prostate cancer. *Science* **329**, 568–571 (2010).
- Wang, X. *et al.* A luminal epithelial stem cell that is a cell of origin for prostate cancer. *Nature* **461**, 495–500 (2009).
- Wang, Z. A. *et al.* Lineage analysis of basal epithelial cells reveals their unexpected plasticity and supports a cell-of-origin model for prostate cancer heterogeneity. *Nat. Cell Biol.* **15**, 274–283 (2013).
- Miyamoto, T., Weissman, I. L. & Akashi, K. AML1/ETO-expressing nonleukemic stem cells in acute myelogenous leukemia with 8;21 chromosomal translocation. *Proc. Natl Acad. Sci. USA* **97**, 7521–7526 (2000).
- Shin, K. *et al.* Hedgehog/Wnt feedback supports regenerative proliferation of epithelial stem cells in bladder. *Nature* **472**, 110–114 (2011).
- Nagao, M., Suzuki, E., Yasuo, K., Yahagi, T. & Seino, Y. Mutagenicity of N-butyl-N-(4-hydroxybutyl)nitrosamine, a bladder carcinogen, and related compounds. *Cancer Res.* **37**, 399–407 (1977).
- Bryan, G. T. The pathogenesis of experimental bladder cancer. *Cancer Res.* **37**, 2813–2816 (1977).
- Hecht, S. S. Cigarette smoking: cancer risks, carcinogens, and mechanisms. *Langenbecks Arch. Surg.* **391**, 603–613 (2006).
- Zeegers, M. P., Tan, F. E., Dorant, E. & van Den Brandt, P. A. The impact of characteristics of cigarette smoking on urinary tract cancer risk: a meta-analysis of epidemiologic studies. *Cancer* **89**, 630–639 (2000).
- Bryan, G. T. Pathogenesis of human urinary bladder cancer. *Environ. Health Perspect.* **49**, 201–207 (1983).
- Spruck, C. H., 3rd *et al.* Two molecular pathways to transitional cell carcinoma of the bladder. *Cancer Res.* **54**, 784–788 (1994).
- Chan, K. S. *et al.* Identification, molecular characterization, clinical prognosis, and therapeutic targeting of human bladder tumor-initiating cells. *Proc. Natl Acad. Sci. USA* **106**, 14016–14021 (2009).
- He, X. *et al.* Differentiation of a highly tumorigenic basal cell compartment in urothelial carcinoma. *Stem Cells* **27**, 1487–1495 (2009).
- Yamaizumi, M., Mekada, E., Uchida, T. & Okada, Y. One molecule of diphtheria toxin fragment A introduced into a cell can kill the cell. *Cell* **15**, 245–250 (1978).
- Maxwell, F., Maxwell, I. H. & Glode, L. M. Cloning, sequence determination, and expression in transfected cells of the coding sequence for the tox 176 attenuated diphtheria toxin A chain. *Mol. Cell Biol.* **7**, 1576–1579 (1987).
- Wu, S., Wu, Y. & Capocchi, M. R. Motoneurons and oligodendrocytes are sequentially generated from neural stem cells but do not appear to share common lineage-restricted progenitors *in vivo*. *Development* **133**, 581–590 (2006).
- Jost, S. P. Cell cycle of normal bladder urothelium in developing and adult mice. *Virchows Arch. B Cell Pathol. Incl. Mol. Pathol.* **57**, 27–36 (1989).
- Thievensen, I., Wolter, M., Prior, A., Seifert, H. H. & Schulz, W. A. Hedgehog signaling in normal urothelial cells and in urothelial carcinoma cell lines. *J. Cell. Physiol.* **203**, 372–377 (2005).
- Kimura, F. *et al.* Decrease of DNA methyltransferase 1 expression relative to cell proliferation in transitional cell carcinoma. *Int. J. Cancer [J. International du Cancer]* **104**, 568–578 (2003).
- Sidransky, D. *et al.* Clonal origin bladder cancer. *N. Engl. J. Med.* **326**, 737–740 (1992).
- Simon, R. *et al.* Cytogenetic analysis of multifocal bladder cancer supports a monoclonal origin and intraepithelial spread of tumor cells. *Cancer Res.* **61**, 355–362 (2001).
- Fadl-Elmula, I. *et al.* Cytogenetic monoclonality in multifocal uroepithelial carcinomas: evidence of intraluminal tumour seeding. *British J. Cancer* **81**, 6–12 (1999).
- Yamamoto, S., Tatematsu, M., Yamamoto, M., Fukami, H. & Fukushima, S. Clonal analysis of urothelial carcinomas in C3H/HeN->BALB/c chimeric mice treated with N-butyl-N-(4-hydroxybutyl)nitrosamine. *Carcinogenesis* **19**, 855–860 (1998).
- Hafner, C. *et al.* Evidence for oligoclonality and tumor spread by intraluminal seeding in multifocal urothelial carcinomas of the upper and lower urinary tract. *Oncogene* **20**, 4910–4915 (2001).
- Trkova, M. *et al.* Analysis of genetic events in 17p13 and 9p21 regions supports predominant monoclonal origin of multifocal and recurrent bladder cancer. *Cancer Lett.* **242**, 68–76 (2006).
- Duggan, B. J. *et al.* Oligoclonality in bladder cancer: the implication for molecular therapies. *J. Urol.* **171**, 419–425 (2004).
- Dahse, R., Gartner, D., Werner, W., Schubert, J. & Junker, K. P53 mutations as an identification marker for the clonal origin of bladder tumors and its recurrences. *Oncol. Rep.* **10**, 2033–2037 (2003).
- Paiss, T. *et al.* Some tumors of the bladder are polyclonal in origin. *J. Urol.* **167**, 718–723 (2002).
- Vriesema, J. L., Aben, K. K., Witjes, J. A., Kiemeny, L. A. & Schalken, J. A. Superficial and metachronous invasive bladder carcinomas are clonally related. *Int. J. Cancer* **93**, 699–702 (2001).
- Rinkevich, Y., Lindau, P., Ueno, H., Longaker, M. T. & Weissman, I. L. Germ-layer and lineage-restricted stem/progenitors regenerate the mouse digit tip. *Nature* **476**, 409–413 (2011).
- Hisha, H. *et al.* Establishment of a novel lingual organoid culture system: generation of organoids having mature keratinized epithelium from adult epithelial stem cells. *Sci. Rep.* **3**, 3224 (2013).
- Yanai, H., Tanaka, T. & Ueno, H. Multicolor lineage tracing methods and intestinal tumors. *J. Gastroenterol.* **48**, 423–433 (2013).
- Montironi, R., Mazzucchelli, R., Lopez-Beltran, A., Cheng, L. & Scarpelli, M. Mechanisms of disease: high-grade prostatic intraepithelial neoplasia and other proposed preneoplastic lesions in the prostate. *Nat. Clin. Practice Urol.* **4**, 321–332 (2007).
- Ayala, A. G. & Ro, J. Y. Prostatic intraepithelial neoplasia: recent advances. *Arch. Pathol. Lab Med.* **131**, 1257–1266 (2007).
- Scarlett, C. J., Salisbury, E. L., Biankin, A. V. & Kench, J. Precursor lesions in pancreatic cancer: morphological and molecular pathology. *Pathology* **43**, 183–200 (2011).
- Maitra, A., Fukushima, N., Takaori, K. & Hruban, R. H. Precursors to invasive pancreatic cancer. *Adv. Anat. Pathol.* **12**, 81–91 (2005).
- Allred, D. C. Ductal carcinoma *in situ*: terminology, classification, and natural history. *J. Natl Cancer Inst. Monogr.* **2010**, 134–138 (2010).
- Fearon, E. R. & Vogelstein, B. A genetic model for colorectal tumorigenesis. *Cell* **61**, 759–767 (1990).
- Hoglund, M. Bladder cancer, a two phased disease? *Semin. Cancer Biol.* **17**, 225–232 (2007).
- Cheng, L. *et al.* Precise microdissection of human bladder carcinomas reveals divergent tumor subclones in the same tumor. *Cancer* **94**, 104–110 (2002).
- Slaughter, D. P., Southwick, H. W. & Smejkal, W. Field cancerization in oral stratified squamous epithelium; clinical implications of multicentric origin. *Cancer* **6**, 963–968 (1953).
- Forsti, A., Louhelainen, J., Soderberg, M., Wijkstrom, H. & Hemminki, K. Loss of heterozygosity in tumour-adjacent normal tissue of breast and bladder cancer. *Eur. J. Cancer* **37**, 1372–1380 (2001).
- Prevo, L. J., Sanchez, C. A., Galipeau, P. C. & Reid, B. J. p53-mutant clones and field effects in Barrett's esophagus. *Cancer Res.* **59**, 4784–4787 (1999).

METHODS

Mice. For lineage tracing experiments, *Shh*^{CreER/WT} mice were mated with the *R26*^{mTmG/mTmG} strain to obtain *Shh*^{CreER/WT}; *R26*^{mTmG/WT} mice. For cell ablation experiments, *Shh*^{CreER/WT} mice were mated with the *R26*^{DTA/WT} strain to obtain *Shh*^{CreER/WT}; *R26*^{DTA/WT} mice. For cancer clonality studies, TM-activated Cre combined with *R26*^{Rainbow/WT} was used to mark cells and their progeny with one of four fluorescence colours. All mouse strains except for Rainbow mice were obtained from Jackson Laboratories. Male mice at 8–10 weeks of age at the beginning of BBN treatment were used. For each experiment, no statistical method was used to predetermine sample size, and mice in each cage were randomly selected for drug/TM or control treatments. The investigators were blinded to allocation during experiments and outcome assessment. Histological assessment of bladder tissue sections was blinded to ensure that the pathologist who assessed the tissues did not know which treatment group each sample belonged to. Mouse procedures were performed under isoflurane anaesthesia, which was administered in a fume hood with a standard vaporizer (J.B. Baulch and Associates). All procedures were performed under a protocol approved by the Administrative Panel on Laboratory Animal Care at Stanford University.

BBN-induced bladder carcinogenesis. A 0.1% concentration of BBN (TCI America) was dissolved in drinking water, and BBN-containing water was provided to mice *ad libitum* for 4–6 months in a dark bottle. BBN-containing water was changed twice a week. Bladders were collected and analysed after 4–6 months of BBN administration.

Lineage tracing studies. For lineage marking of *Shh*-expressing basal cells before BBN exposure, *Shh*^{CreER/WT}; *R26*^{mTmG/WT} mouse strains were injected intraperitoneally with 4 mg of TM per 30 g body weight daily for 3 consecutive days. BBN-containing water was provided to mice *ad libitum* for 4 or 6 months beginning 5 days after the last TM injection. Mice were euthanized and bladders dissected for further analysis. For marking and tracing of *Shh*-expressing hyperplastic cells, *Shh*^{CreER/WT}; *R26*^{mTmG/WT} mice were exposed to BBN for 4 months and then injected intraperitoneally with 4 mg of TM (per 30 g body weight) daily for 3 consecutive days. Mice were then provided with BBN-containing water for an additional 2 months, euthanized and bladders dissected for further analysis. To label *Shh*-expressing cells in invasive carcinoma, *Shh*^{CreER/WT}; *R26*^{mTmG/WT} mouse strains were provided with BBN-containing water for 6 months and then injected intraperitoneally with 4 mg of TM (per 30 g body weight) daily for 3 consecutive days. Mice were euthanized 5 days after the last TM injection, and bladders were analysed. To label *Shh*-expressing cells in CIS lesions, *Shh*^{CreER/WT}; *R26*^{mTmG/WT} mouse strains were provided with BBN-containing water for 4 months and then injected intraperitoneally with 4 mg of TM (per 30 g body weight) daily for 3 consecutive days before mice were euthanized. For cancer clonality studies, *Actin*^{CreER/WT}; *R26*^{RAINBOW/WT} mouse strains were injected with 2 mg of TM (per 30 g body weight) before BBN exposure. Note that owing to poor expression of *Actin*^{CreER}, bladder stromal cells retain the original expression of EGFP.

Cell ablation studies. For ablation of *Shh*-expressing cells before BBN exposure, *Shh*^{CreER/WT}; *R26*^{DTA/WT} mice were injected intraperitoneally with 4 mg of TM (per 30 g body weight) daily for 5 consecutive days. Bladders then were examined for ablation of basal cells 5 days after the last TM injection. For studies on the effect of basal cell loss on bladder tumorigenesis, BBN-containing water was provided to

mice *ad libitum* for 4–6 months after basal cell ablation by daily TM injection for 5 days as described above. Mice were then euthanized and bladders then dissected for further analysis.

Immunofluorescence analysis. Bladders were dissected and embedded in OCT compound for snap freezing (Tissue-Tek). Frozen blocks were sectioned at 10 mm intervals using a Microm cryostat. For immunostaining, frozen tissue sections were fixed in 4% paraformaldehyde for 30 min at 4 °C. After washing three times with PBS, tissue sections were blocked in 2% goat serum in PBS containing 0.25% Triton X-100 for 1 h, and incubated with primary antibodies diluted in blocking solution overnight at 4 °C in a humidified chamber (rabbit anti-CK5, 1:300 dilution, ab53121 from Abcam; rat anti-CK18/8, 1:300 dilution, Troma-1 from hybridoma bank; rabbit anti-GFP, 1:1,000 dilution, A-11122 from Invitrogen). Sections were washed three times with PBS containing 0.25% Triton X-100, incubated with DAPI and appropriate Alexa fluor 488-, 594- or 633-conjugated secondary antibodies diluted 1:1,000 in blocking solution for 2 h at room temperature, washed again three times, and mounted on slides with Prolong Gold mounting reagent (Invitrogen). All images were obtained using a Zeiss LSM 510 inverted confocal microscope and prepared for publication with Zeiss LSM 5 Image Browser software and Adobe Photoshop CS3.

Laser capture microdissection. For laser capture microdissection (LCM), bladder sections were prepared using an LCM staining kit (Ambion) and a Leica LMD6000 Laser Microdissection Microscope. After LCM, total RNA was prepared using RNAqueous-Micro RNA isolation kit (Ambion). Quantitative PCR with reverse transcription was performed using iScript one-step RT-PCR kit with SYBR Green and the Bio-Rad iCycler (BioRad). All values were normalized to the HPRT internal control.

Tumour transplantation. Bladder tumours were minced, and then incubated with Liberase blendzymes 2 and 4 (Roche) in DMEM (Invitrogen) at 37 °C for 3 h. A single-cell suspension was obtained by 10 min of trituration every 30 min during this incubation, followed by filtration through 70 µm cell strainers. After the lysis of red blood cells, cells were washed with HBSS/2% fetal bovine serum and were counted using a haemocytometer (Hausser Scientific). Cells were resuspended in 100 µl HBSS containing 30% Matrigel (BD Bioscience) and then injected with 31-gauge insulin syringes (Becton Dickinson) subcutaneously into the flanks of anaesthetized NSG mice (Jackson Laboratories). For the transplantation of genetically labelled cells, *Shh*^{CreER/WT}; *R26*^{mTmG/WT} mice were exposed to BBN for 4 months and then injected intraperitoneally with 4 mg of TM per 30 g body weight daily for 3 consecutive days. Mice were provided with BBN-containing water for an additional 2 months. Bladder tumours from resulting mice were dissociated as described above. Cells were sorted using a FACS AriaII cytometer (BD Biosciences), and analysis of flow cytometry data was performed using FlowJo Software (TreeStar). FACS-sorted mG-positive and mT-positive cancer cells were separately injected into NSG mice as described above. For the transplantation of mixed cells, FACS-sorted mG-positive and mT-positive cancer cells were mixed in 100 µl HBSS containing 30% Matrigel (BD Bioscience). The mixed cell suspension was injected into NSG mice as described above. For the orthotopic model, mG/EpCAM- and mT/EpCAM-positive cells were FACS-sorted and injected submucosally into the anterior aspect of the bladder dome. Abdominal incisions were then closed with 4–0 Vicryl suture, and the surgical site was treated once with topical antibiotic ointment.

ERRATUM

Cellular origin of bladder neoplasia and tissue dynamics of its progression to invasive carcinoma

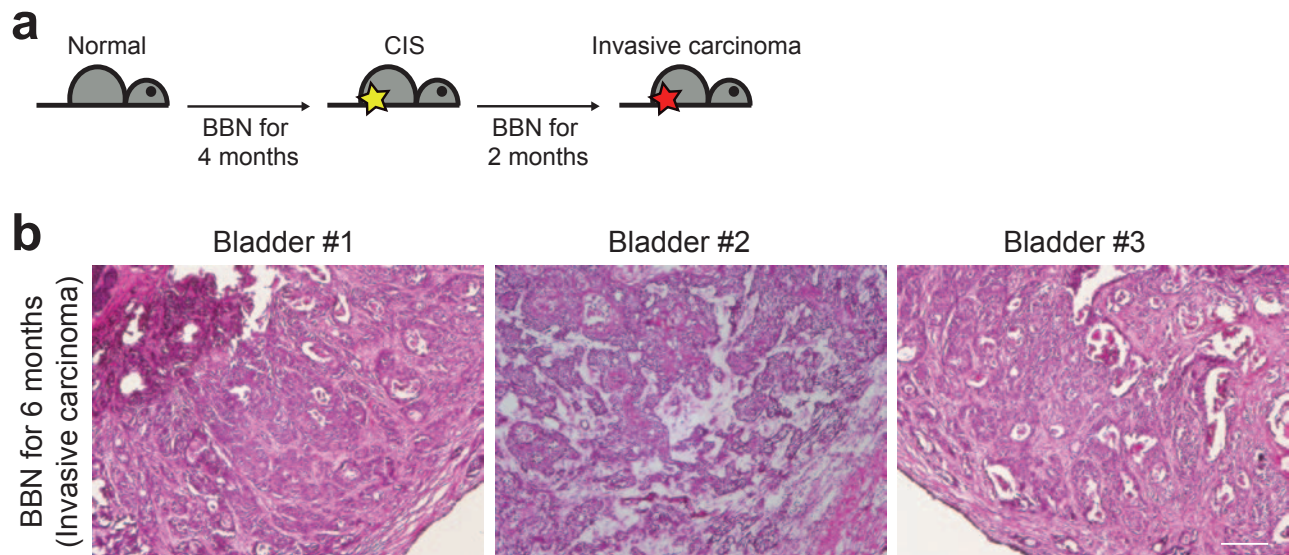
Kunyoo Shin, Agnes Lim, Justin I. Odegaard, Jared D. Honeycutt, Sally Kawano, Michael H. Hsieh and Philip A. Beachy

Nat. Cell Biol. **16**, 469–478 (2014); published online 20 April 2014; corrected after print 24 April 2014

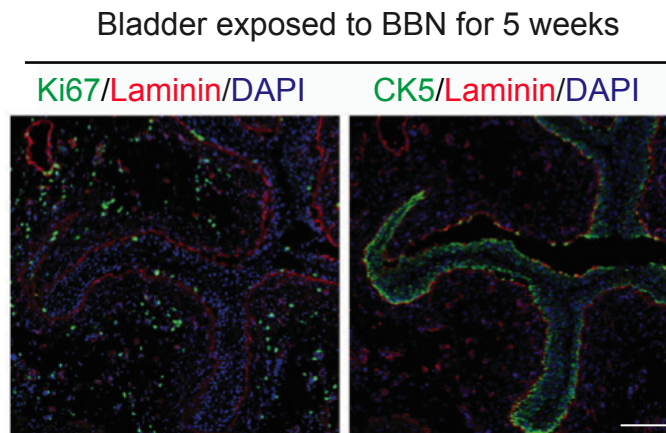
In the version of this Article originally published, the bottom panel of Fig. 4b should have read: '*Shh*^{CreER/WT}; *R26*^{DTA/WT} (tamoxifen)'.

In Fig. 7a the three shaded triangles on the left should have been in the sequence: dark, intermediate, light. These errors have now been corrected in the online versions of the Article.

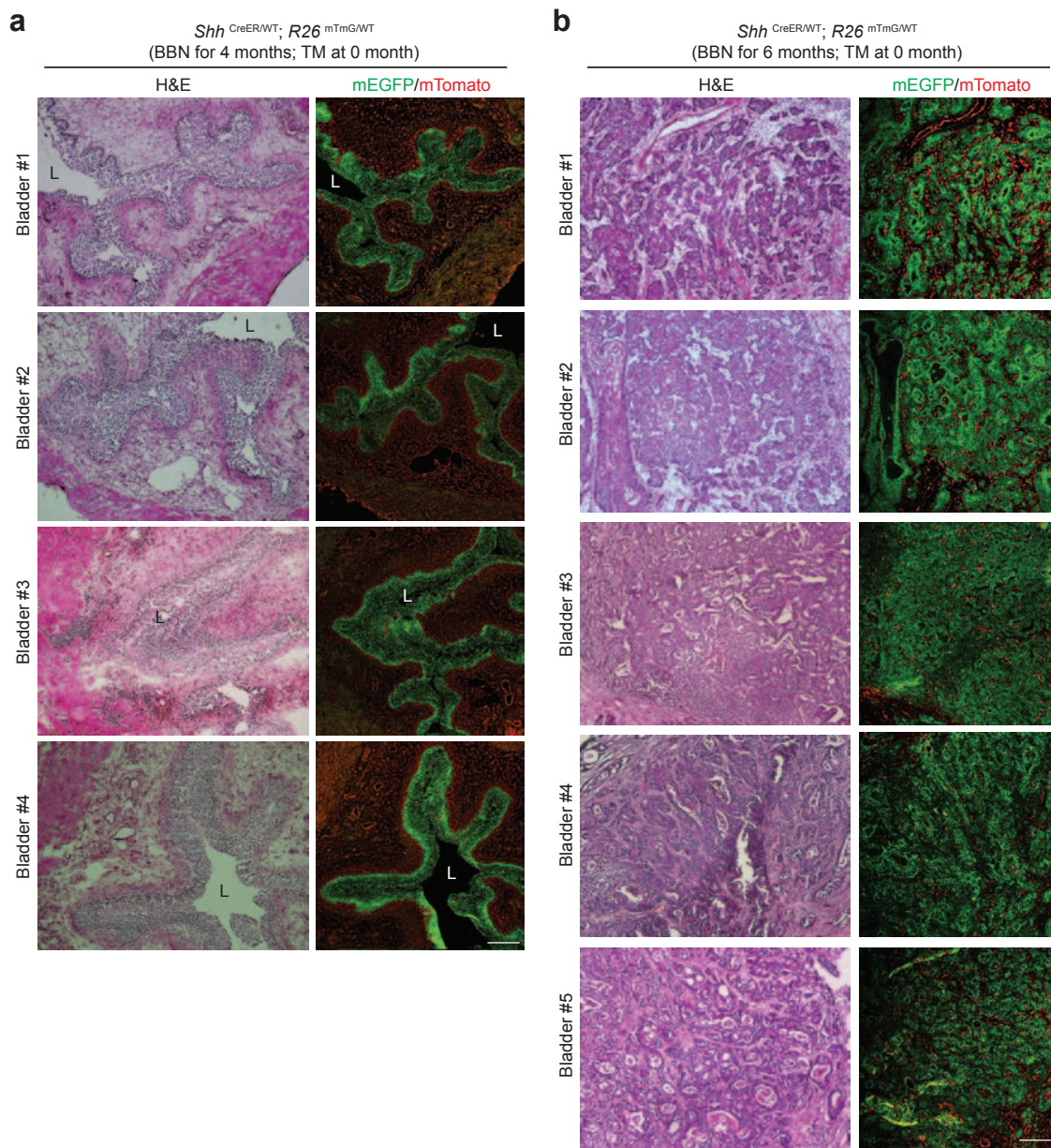
DOI: 10.1038/ncb2956



Supplementary Figure 1 Mouse model of bladder cancer. **(a)** Schematic diagram describing mouse model of BBN-induced bladder cancer. **(b)** Histopathological analysis (H&E) of invasive carcinoma after 6 months of BBN exposure from three different animals. Scale bars represent 50 μ m

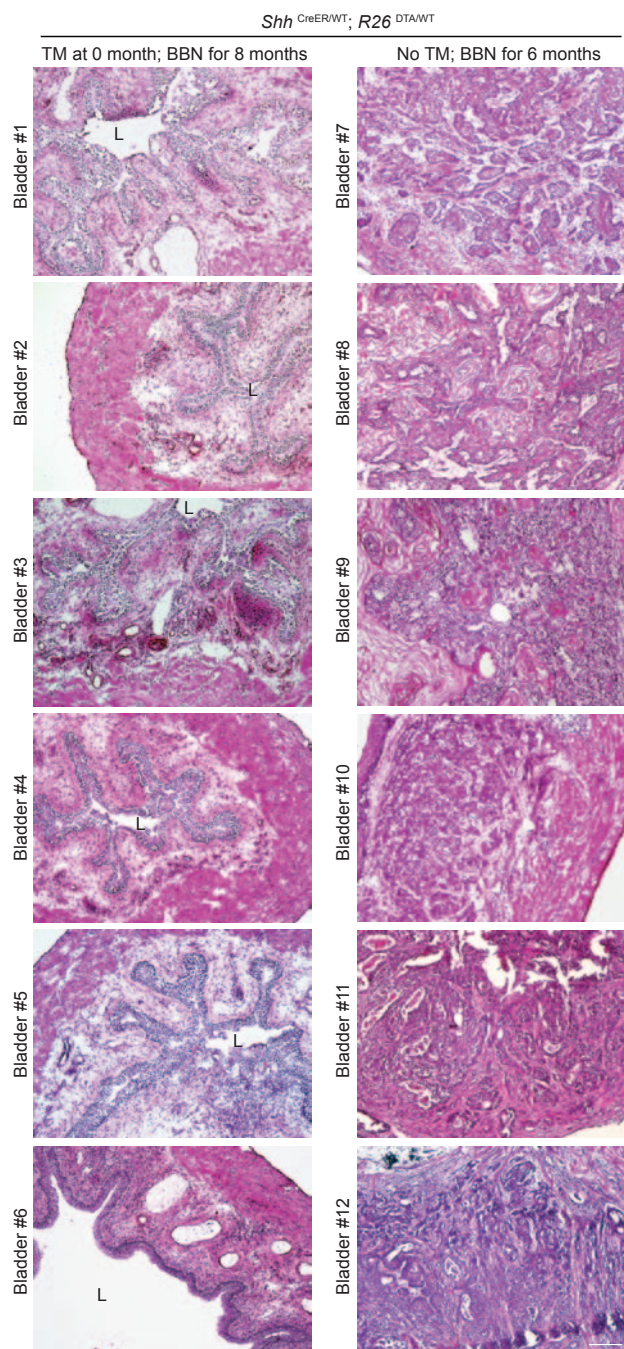


Supplementary Figure 2 Lack of urothelial proliferation at early stages of BBN exposure. Serial sections made from bladder exposed to BBN for 5 weeks were stained with Ki67 (left panel, green) and CK5 (right panel, green). Sections were co-stained with laminin (red) and DAPI (blue). Scale bars represent 50 μ m.



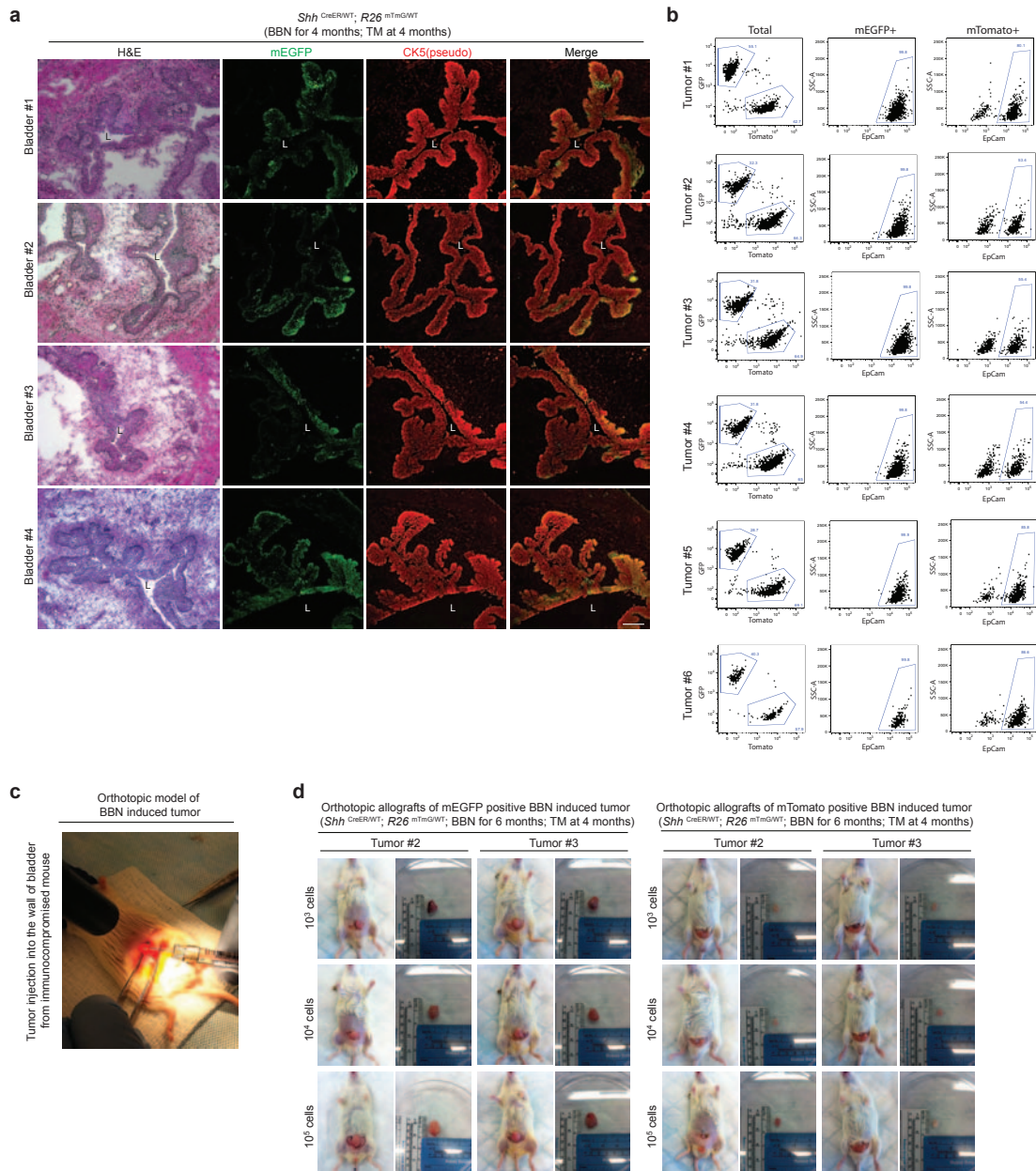
Supplementary Figure 3 Marked *Shh*-expressing basal stem cells give rise to CIS and invasive carcinoma. **(a)** *Shh*^{CreER}; *R26*^{mTmG} mice (four different animals, bladder #1-4) injected with TM on three consecutive days were exposed to BBN for 4 months to induce development of CIS and bladder tissues analyzed (H&E, left panel; mG/mT expression, right panel). **(b)**

Shh^{CreER}; *R26*^{mTmG} mice (five different animals, bladder #1-5) injected with TM on three consecutive days were exposed to BBN for 6 months and bladder tumors analyzed (H&E, left panels; mG/mT expression, right panels). L, bladder lumen. Representative images are shown in Figure 2. Scale bars represent 50µm.



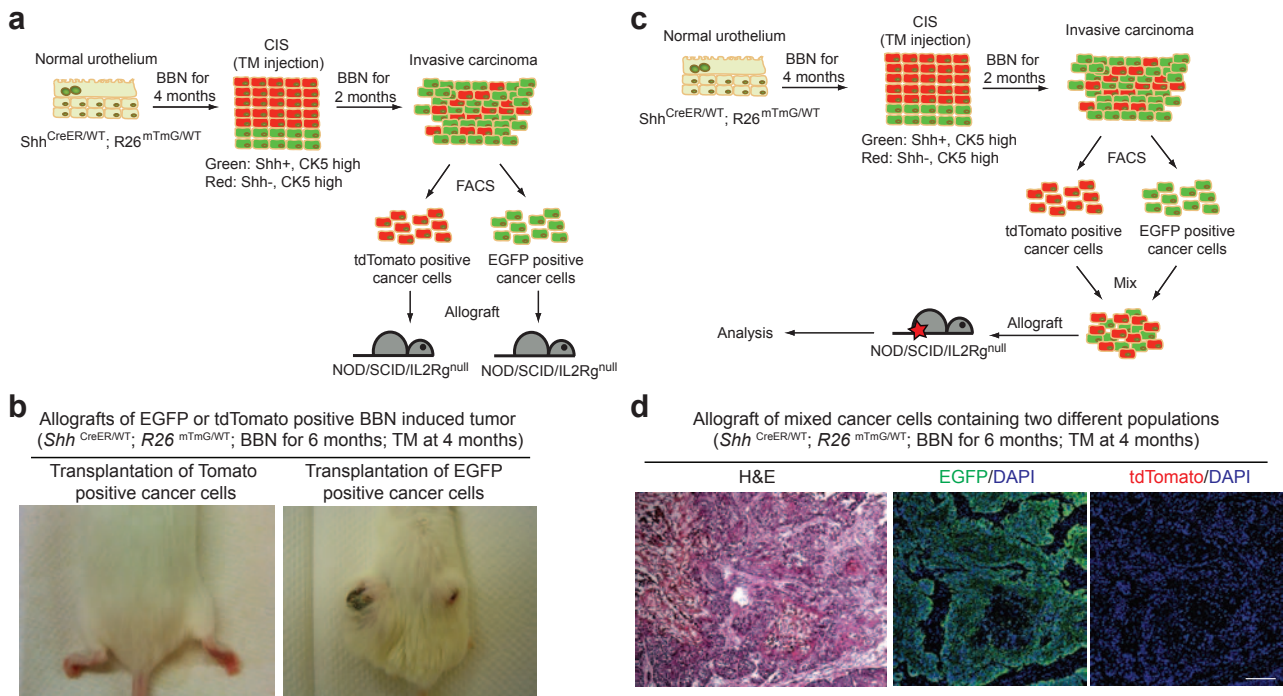
Supplementary Figure 4 Ablation of *Shh*-expressing basal cells renders bladder resistant to nitrosamine-induced formation of invasive carcinoma. TM was injected into *Shh*^{CreER}; *R26*^{DTA} mice (twelve different animals; bladder #1-6, with TM; bladder #7-12, without TM) on five consecutive days to

ablate *Shh*-expressing basal cells, and these mice subsequently were exposed to BBN for 6 months (right panels; without TM) and 8 months (left panels; with TM). Bladder tissues were analyzed by H&E staining. L, bladder lumen. Representative images are shown in Figure 3c. Scale bars represent 50µm.



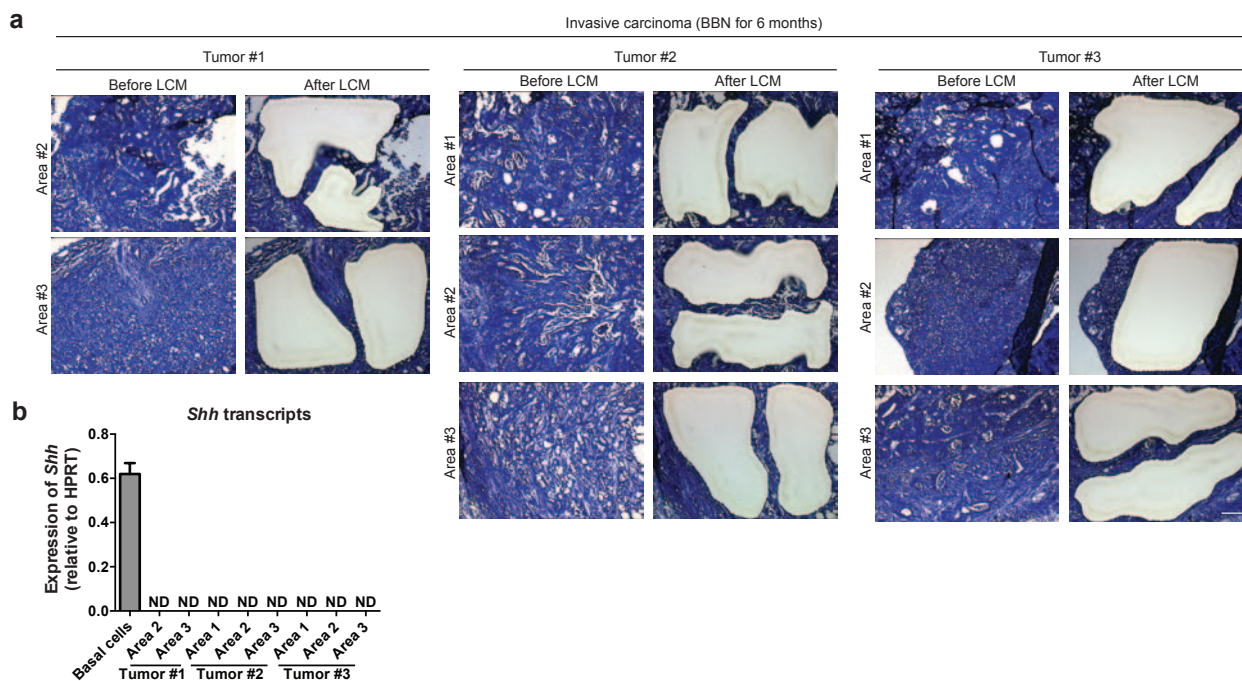
Supplementary Figure 5 Tumor-propagating cells derive exclusively from *Shh*-positive cells in the CIS lesion. **(a)** *Shh^{CreER}; R26^{mTomG}* mice (four different animals: Bladder #1-4) were exposed to BBN for 4 months to induce development of CIS. TM was injected on three consecutive days to label *Shh*-expressing CIS cells prior to sacrifice and analysis of bladder tissues by H&E staining (left panel) or by immunostaining for mG and CK5 (green and red, respectively, in three right panels). L, bladder lumen. **(b)** mG/EpCAM-positive

and mT/EpCAM-positive populations from six different invasive carcinomas generated as described in Fig. 5b were separated using FACS. **(c)** BBN-induced bladder tumor cells were injected intramurally into the dome of the bladder. **(d)** Orthotopic transplantation with serial dilutions of mG/EpCAM-positive and mT/EpCAM-positive cells from invasive carcinomas #2 and #3 (invasive carcinoma #1 is shown in Fig. 5e). Representative images for (a) and (d) are shown in Figure 5a, and 5e, respectively. Scale bars represent 50µm.



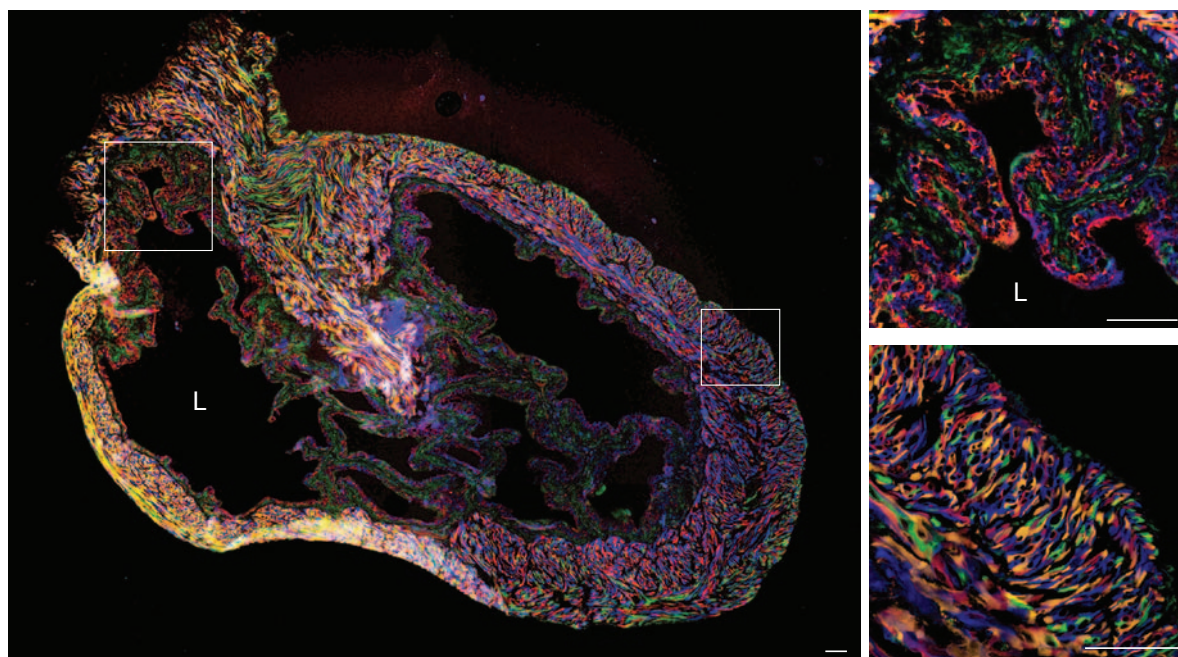
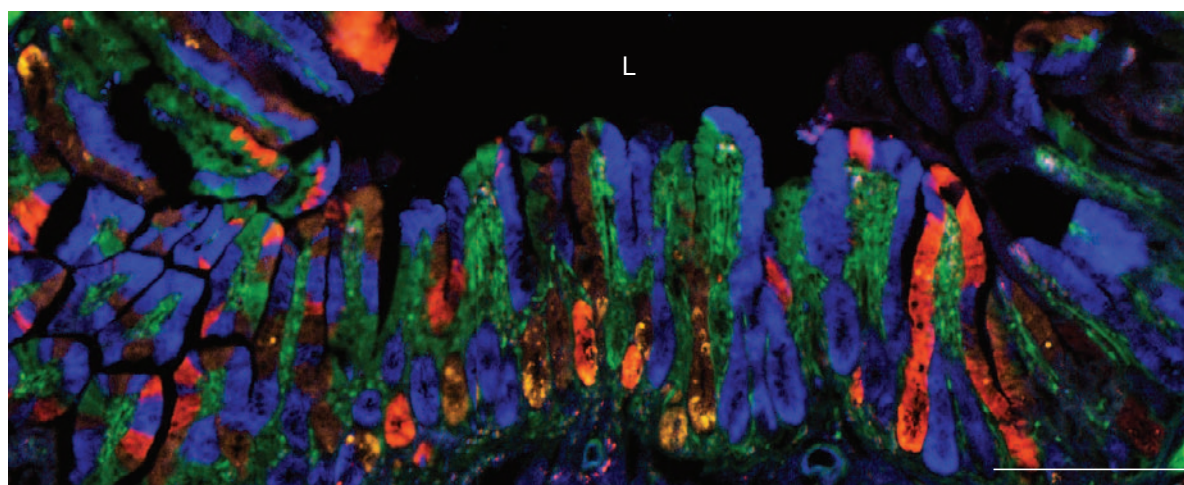
Supplementary Figure 6 *Shh*-negative cells in CIS lesion do not contribute to tumor-propagating cells in invasive carcinoma. **(a)** $Shh^{CreER}; R26^{mTmG}$ mice were exposed to BBN for 4 months to induce CIS lesions, then injected with TM on three consecutive days, which heritably labels *Shh*-positive cells with EGFP whereas cells that do not express *Shh* remain labeled with tdTomato. Mice were subsequently treated with BBN for two more months, and EGFP and tdTomato positive cancer cells in invasive carcinoma from the resulting animals were separated by FACS. EGFP and tdTomato positive cells were then transplanted subcutaneously into immunocompromised mice ($NOD/SCID/IL2Rg^{null}$). **(b)** Allografts from transplantation of tdTomato- and EGFP-positive cells are shown in left and right panels, respectively. **(c)** Experimental strategy to investigate the tumorigenic capacity of mixed cancer cells originating

from *Shh*-positive or -negative CIS cells. $Shh^{CreER}; R26^{mTmG}$ mice were treated with BBN for 4 months to induce CIS, then injected with TM on three consecutive days to mark *Shh*-positive and -negative cells with EGFP and tdTomato, respectively. Mice were subsequently treated with BBN for two more months, and EGFP- and tdTomato-positive cancer cells from the resulting animals were separated by FACS. Equal numbers of EGFP- and tdTomato-positive cells were then mixed and subcutaneously transplanted into immunocompromised mice ($NOD/SCID/IL2Rg^{null}$). **(d)** Allograft tumor from the experiment described in **(c)** was analyzed by H&E staining (left panel) and immunostaining for EGFP and tdTomato (green and red, respectively in middle and right panels). Note only EGFP, not tdTomato, is expressed in the tumor allograft. Scale bar represents 50 μ m.



Supplementary Figure 7 Loss of *Shh* expression in invasive carcinoma. **(a)** Laser capture microdissection of three different tumor areas from three distinct bladder tumors. Nine tumor areas were assessed; 3 different tumor areas from 3 distinct tumors. Representative images (area #1 from tumor #1) are shown in

Figure 6c. **(b)** Analysis of *Shh* mRNA expression by qRT-PCR in microdissected basal urothelium and carcinoma cells. ND, not detected. Data are presented as mean \pm s.e.m from 3 technical replicates; 9 tumor areas were assessed (3 different tumor areas from 3 distinct tumors). Scale bars represent 50 μ m.

a *Actin*^{CreER/WT}; *R26*^{Rainbow/WT} (Bladder at 0 month; TM at 0 month)

b *Actin*^{CreER/WT}; *R26*^{Rainbow/WT} (Intestine at 4 months; TM at 0 month)


Supplementary Figure 8 Stochastic four color fluorescence marking of normal bladder and intestinal cells. **(a)** TM was injected into *Actin*^{CreER}; *R26*^{Rainbow} mouse to label all cells in the bladder with one of four fluorescence colors prior to BBN exposure. Right panels show magnified views of the regions

highlighted by white boxes in the left panel. **(b)** Mouse intestine 4 months after TM injection into *Actin*^{CreER}; *R26*^{Rainbow} mouse. Note clonal expansions of intestinal stem cells from crypts into the villi, as expected, thus validating four-color marking with the Rainbow mouse. L, lumen. Scale bars represent 50 μ m.

Supplementary Table 1 Histopathology of BBN-exposed bladder

Sample number	Time of BBN exposure			
	1month	2months	3months	4months
#1	No CIS	No CIS	No CIS	Widespread CIS (>30%)
#2	No CIS	No CIS	No CIS	Widespread CIS (>30%)
#3	No CIS	No CIS	Focal CIS (<10%)	Scattered CIS (10-30%)
#4	No CIS	No CIS	Focal CIS (<10%)	Scattered CIS (10-30%)
#5	N/A	N/A	Scattered CIS (10-30%)	Widespread CIS (>30%)
#6	N/A	N/A	Widespread CIS (>30%)	Widespread CIS (>30%)
#7	N/A	N/A	Scattered CIS (10-30%)	Widespread CIS (>30%)

Supplementary Table 2 Histopathology of BBN-exposed bladder from vehicle-treated *Shh*^{CreER}; *R26*^{DTA} mice

Sample number	Time of BBN exposure			
	1month	2months	3months	4months
#1	No CIS	No CIS	No CIS	Scattered CIS (10-30%)
#2	No CIS	Focal CIS	No CIS	Scattered CIS (10-30%)
#3	No CIS	No CIS	Focal CIS (<10%)	Scattered CIS (10-30%)
#4	No CIS	No CIS	Focal CIS (<10%)	Widespread CIS (>30%)
#5	N/A	N/A	Focal CIS (<10%)	Widespread CIS (>30%)
#6	N/A	N/A	Scattered CIS (10-30%)	Widespread CIS (>30%)
#7	N/A	N/A	Scattered CIS (10-30%)	Widespread CIS (>30%)
#8	N/A	N/A	Scattered CIS (10-30%)	Widespread CIS (>30%)

Supplementary Table 3 Histopathology of BBN-exposed bladder from tamoxifen-treated *Shh*^{CreER}; *R26*^{DTA} mice

Sample number	Time of BBN exposure			
	1month	2months	3months	4months
#1	No CIS	No CIS	No CIS	No CIS
#2	No CIS	No CIS	No CIS	No CIS
#3	No CIS	No CIS	No CIS	No CIS
#4	No CIS	No CIS	No CIS	No CIS
#5	N/A	N/A	No CIS	Widespread CIS (>30%)
#6	N/A	N/A	Focal CIS (<10%)	Widespread CIS (>30%)
#7	N/A	N/A	No CIS	Widespread CIS (>30%)
#8	N/A	N/A	Focal CIS (<10%)	No CIS
#9	N/A	N/A	N/A	No CIS